Interplay between purging and admixture shapes genetic load in an invasive guppy population

Katarzyna Burda[1], Mary J Janecka[2], Ryan S. Mohammed[3,4], David R. Clark[5], Rachael Kramp[5], Jessica F. Stephenson[6], Jacek Radwan[1], Mateusz Konczal[1*]

[1] Evolutionary Biology Group, Faculty of Biology, Adam Mickiewicz University; 60-614 Poznań, Poland

[2] Carnegie Museum of Natural History, Powdermill Nature Reserve, Rector, Pennsylvania, USA

[3] College of Science and Mathematics, Auburn University, Auburn, Alabama, USA

[4] Department of Life Sciences, Faculty of Science and Technology, The University of the West Indies, Trinidad and Tobago.

[5] Department of Biological Sciences, University of Pittsburgh, Pittsburgh, Pennsylvania, USA

[6] Department of Zoology, Stockholm University, Stockholm 106 91, Sweden

*mateusz.konczal@amu.edu.pl

Abstract

Demographic history can shape the genetic load of populations by influencing the efficacy of selection, levels of heterozygosity, and by incorporation of new variants via gene flow. Understanding these dynamics is crucial for identifying threats to population viability and predicting evolutionary trajectories of invasive populations translocated by humans into non-native environments. We investigated these processes in Trinidadian guppies (*Poecilia reticulata*) by estimating genetic loads in multiple populations, with a particular focus on a single expanding population where translocated individuals have rapidly spread and replaced native populations. Overall, we observed the expected negative relationship between neutral genetic diversity and relative genetic load. In the translocated population, patterns differed between strongly and weakly deleterious mutations. Strongly deleterious alleles were purged at the isolated translocation site but tended to accumulate along the expansion front. In contrast, genetic load estimated based on weakly deleterious variants declined along the expansion gradient. These differing patterns can be explained by admixture with native populations (which carried fewer weakly deleterious mutations) reducing the overall genetic load of the population at the expansion front. However, admixture also increased genetic diversity and introduced new strongly deleterious alleles, which reversed the effect of purging. Together, our findings illustrated the complex interactions determining genetic load in subdivided populations, offering important insights into the evolutionary aspects of biological invasions.

1. Introduction

Genetic load refers to the fitness decrease due to the presence of deleterious variants in a genome (Crow 1989; Bertorelle et al. 2022). Most of the deleterious mutations have slight effects in heterozygous carriers and remain rare in large panmictic populations (Eyre-Walker and Keightley 2007). Such deleterious variants present in heterozygous genotypes are often referred to as "masked genetic load" (Bertorelle et al. 2022). Under some demographic scenarios, deleterious variants can increase in frequency and become exposed in homozygotes as a "realized genetic load", which may threaten population survival. In such a situation, deleterious alleles may either become common, or even fixed, in a population decreasing its mean fitness, or they may be eliminated from the population by "purging" (Dussex et al. 2023; Robinson et al. 2023).

Demographic changes, such as an event reducing population size, are expected to affect genetic variation and the genetic load of a population through greater genetic drift (Wright 1932) and inbreeding (Wright 1922). Genetic drift increases the variance around the mean frequency of deleterious mutations, allowing some deleterious alleles to drift to high frequencies (Stewart et al. 2017; de Pedro et al. 2021; Zeitler et al. 2023). Thus, in small populations in which selection fails to remove deleterious mutations of weak effects, these variants accumulate over time (Kimura and Ohta 1969) and may eventually fix (Kimura et al. 1963). This accumulation reduces fitness, which may further reduce population size, potentially resulting in a vicious circle of "mutational meltdown" (Lynch et al. 1995). Under this scenario, such "genetic erosion" in small, isolated populations of endangered species should relate to their estimated neutral genetic variation, reflecting "effective population size". In other words, genome-wide genetic variation may be crucial information for conservation (Kardos et al. 2021). Consistent with these theoretical predictions, a negative relationship between neutral nucleotide diversity and realized load (or drift load) was indeed found, for example in an endangered rattlesnake (Mathur et al. 2023).

However, the relationship between genetic load and neutral diversity depends on their values (Mathur et al. 2023) and may be changed by recent demographic events. For instance, a transient recent population size reduction might increase a population's mean fitness through several processes. First, alleles at low frequencies, such as strongly deleterious mutations, are likely to be lost by drift. Second, reduced population size increases the probability that alleles carried by mating partners are identical by descent, leading to increased homozygosity in a population (Wright 1922) thus changing masked load into realized load. Highly deleterious variants at low frequencies in pre-bottleneck population thus become exposed to natural selection (Charlesworth and Willis 2009). If selection can overcome genetic drift, it may purge such large effect deleterious variants, ultimately decreasing both masked and total genetic load (Barrett and Charlesworth 1991; Crnokrak and Barrett 2002; Keller and Waller 2002; Glémin 2003). Purging can reduce a population's extinction risk and potentially explain observations of small populations persisting for long periods of time despite low genetic variation (Robinson et al. 2016; Dehasque et al. 2023). New genomic data suggest that purging occurs more often than previously thought (Dussex et al. 2023), however, its effectiveness differs between populations and species (Lan et al. 2025). Consequently, Teixeira and Huber (2021) argued against the importance of neutral genetic diversity for the conservation of wild populations, and instead advocated for better understanding the properties of non-neutral genetic diversity. Despite wide discussion and studies in multiple systems, there is still no general understanding of its value for

conserving wild populations (Robinson et al. 2019; Ralls et al. 2020; Kardos et al. 2021; Kyriazis et al. 2021; van Oosterhout et al. 2022; Kardos et al. 2023).

Such investigations might be also important in the context of biological invasions (Estoup et al. 2016). Even though invasions and endangered species reflect opposite ends of a spectrum of ecological success, they experience similar challenges (Colautti et al. 2017). Both natural and artificial translocations that give rise to invasions usually introduce small numbers of often related individuals, and thus the initial stages of invasion involve small effective population sizes. Maintaining invasive potential despite expected loss of genetic diversity and increased genetic load was termed the "genetic paradox" of invasions (Estoup et al. 2016; Kołodziejczyk et al. 2025). It has been suggested that purging may explain this paradox and contribute to invasive potential of translocated populations (Estoup et al. 2016). Purging in invasive species has, however, been documented in only a few cases (Zayed et al. 2007; Facon et al. 2011; Lombaert et al. 2025), making generalization difficult. Following an initial bottleneck, invasive species often experience rapid range expansion. Such expansions can involve multiple subsequent bottlenecks, increasing the effects of purging and genetic drift especially at the expansion front (Peischl et al. 2015). This process intensifies with extending distance from the expansion source, and might have opposite effects on strongly and weakly deleterious variations, with, respectively purging and accumulation (Rougemont et al. 2023).

However, unlike endangered species, successful invasions are often associated with admixture between diverged genotypes or hybridization between translocated and native populations (Colautti et al. 2017; Barker et al. 2019; Kołodziejczyk et al. 2025). Potential benefits of such admixture include increased genetic variation and incorporation of alleles associated with local adaption into genetic pool of invasive species, enabling adaptation to novel habitats (Wagner et al. 2017; Kołodziejczyk et al. 2025). Interestingly, genetic diversity was not reduced in most genomic studies of invasive populations, probably because of admixture or hybridization (Kołodziejczyk et al. 2025). Little is known about the effect of admixture on the dynamics of genetic load. Admixture might be expected to mask the realized genetic load of expanding population, not only for deleterious mutations that increased in frequency during past bottlenecks, but also ones already fixed in a population. It can also introduce new variants into a population, which can either counteract purging or be deleterious, potentially increasing total genetic load of an invasive population. It has been suggested for example, that introgression of Neanderthal ancestry into anatomically modern human genomes, during the expansion out of Africa, reduced fitness by at least 0.5%, due to increased genetic load derived from Neanderthal genomes (Harris and Nielsen 2016). However, whether such scenarios can affect invasion potential has rarely been studied.

Here, we examine the fate of genetic load during invasion of Trinidadian guppies (*Poecilia reticulata*) into a diverged, allopatric population, during which translocated individuals rapidly spread and replaced native populations. Guppies occur naturally in fresh waters of Trinidad, Tobago and South America, but have been translocated and successfully invaded multiple sites across the globe (Deacon et al. 2011). Natural Trinidadian populations have been intensively studied by generations of ecologists and evolutionary biologists (Magurran 2005) and some of these studies included translocation experiments (Fraser et al. 2015; Fitzpatrick et al. 2016). One of such translocations occurred in the Turure river in 1957 (Endler 1980; Reznick and Bryga 1987; Shaw et al. 1992). Fish from the lower Guanapo River (Caroni drainage) were moved to a site in the upper Turure River (Oropouche drainage) which previously lacked guppies (Magurran 2005). 200 guppies,

approximately half females, were introduced (Shaw et al. 1992; Sievers et al. 2012). Importantly, the source and recipient drainages are inhabited by differentiated guppy populations (Willing et al. 2010), with long separate histories (estimated to have split 0.18-1.2 mya, based on net divergence (Fajen and Breden 1992; Whiting et al. 2021)), and evidence of partial reproductive isolation (Russell and Magurran 2006). The Oropouche fish may be a distinct species, and has been named *P. obscura* (Schories et al. 2009), though evidence for barriers to gene flow is weak (Magurran 2005; Devigili et al. 2018). The differentiation documented by these studies reflects isolation, but also adaptation to different local environments (Reznick et al. 1990; Bassar et al. 2010; Kemp et al. 2018). However, after translocation, genetically foreign individuals spread rapidly, and largely replaced native populations in the lower parts of the Tururе river. Furthermore, several sources of evidence demonstrated ongoing admixture from resident populations (Becher and Magurran 2000; Willing et al. 2010; Sievers et al. 2012).

We aimed to test whether spread of Guanapo-derived genomes into the resident populations of the Tururе River was associated with changes of genetic load. In particular, we test the hypothesis that the Guanapo-derived population introduced into the upstream Tururе was purged of highly deleterious mutations and now has an overall low genetic load, potentially increasing invasive potential (Sievers et al. 2012). To test this hypothesis, we compared the genetic load of the upstream Tururе population with that of the Guanapo source population. Additionally, we explore the accumulation of genetic load along the Tururе river, to test the hypothesis of expansion associated with a series of bottlenecks, allowing the accumulation of weakly deleterious mutations and purging strongly deleterious mutations in downriver sites. However, if admixture occurred along with expansion, as earlier work suggest (Willing et al. 2010; Sievers et al. 2012), the genetic load might also be affected by this process. We therefore explore differences in both genetic load and admixture along the river. Additionally, to provide a benchmark to interpret genetic load in our focal populations, we test for associations between neutral diversity and genetic load using multiple populations from other rivers. Guppy populations in Trinidadian rivers range in population size from hundreds to tens of thousands of individuals (Whiting et al. 2021), providing the opportunity to test for such an association.

2. *Results*

2.1 *Population structure and nucleotide diversity*

We analyzed 201 individuals from 15 populations (sampling sites) originating from 9 rivers on Trinidad (Aripo, Caura, Guanapo, Lopinot, Santa Cruz, La Seiva, Oropouche, Quare, Turure), and 2 rivers on Tobago (Dog River and Roxborough; Fig. 1; Supplementary Table 1). Five analyzed Trinidadian rivers belong to Caroni drainage and the other four to Oropouche drainage. Three rivers were sampled in more than one location: Quare (upper and lower), Oropouche (upper and lower), and Turure (upper, middle and lower). Samples were sequenced yielding mean coverage of 15x (7x - 36x) and were mapped to the reference genome with over 97% reads aligned in all individual sample.

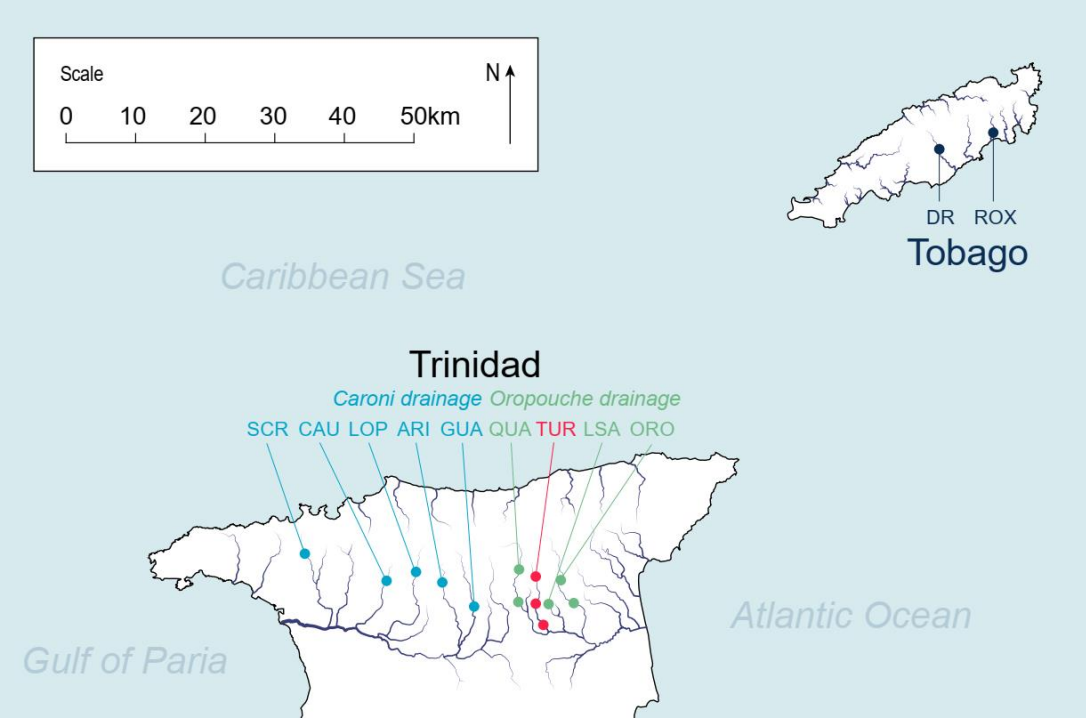

Figure 1. Sampling locations in Trinidad and Tobago, across the rivers: SCR (Santa Cruz), CAU (Caura), LOP (Lopinot), ARI (Aripo), Guanapo (GUA), QUA (Quare), TUR (Turure), LSA (La Seiva), ORO (Oropouche), DR (Dog River), ROX (Roxborough).

We performed principal component analysis (PCA) to understand the overall pattern of genetic differentiation between populations. The first PC (explaining 22.2% variation) separated Oropouche (which included the Turure, recipient river) from the Caroni (which included the Guanapo, source river) drainages, whereas the second, explained 13.8% of variation and separated samples from Trinidad from those on Tobago (Fig.2). Turure individuals cluster with the Guanapo population. Individuals from the lower Quare river sites have intermediate positions on PC1, and cluster with neither Caroni nor other Oropuche drainage individuals, consistent with strong signals already suggested admixture in this population (Willing et al. 2010; Fitzpatrick et al. 2016; Whiting et al. 2021).

Admixture analysis identified the optimal K-value to be 12, with clear differentiation among the two islands and the Trinidad drainages (Fig. 3). The upper and lower Oropouche sites are highly similar

to each other, whilst the upper and lower Quare sites differ, with higher variation in the lower site. In the upper Turure river, to which Caroni drainage fish were translocated, we found high similarity to Guanapo source population and no evidence of admixture, in accordance with previous findings (Willing et al. 2010). As expected, increased admixture is detected downstream, probably reflecting crosses between introduced and native populations, although the vast majority of the ancestry is from the introduced populations (Fig. 3).

Interestingly, we observed 5 individuals from the Turure middle site, that cluster separately from the other samples from the same site (Fig. 2). In the admixture plot they represent pure distinct genetic ancestry, while one other individual from the same population seems to be F1 hybrid, and others seem to be admixed for this ancestry (Fig. 3). These individuals come from two different sampling years, making it unlikely that they represent mislabeling or other errors. Most likely, these individuals represent a true distinct genetic population within this river, possibly due to another recent translocation from an unknown source. These five individuals and the putative F1 hybrid were excluded from the analyses below.

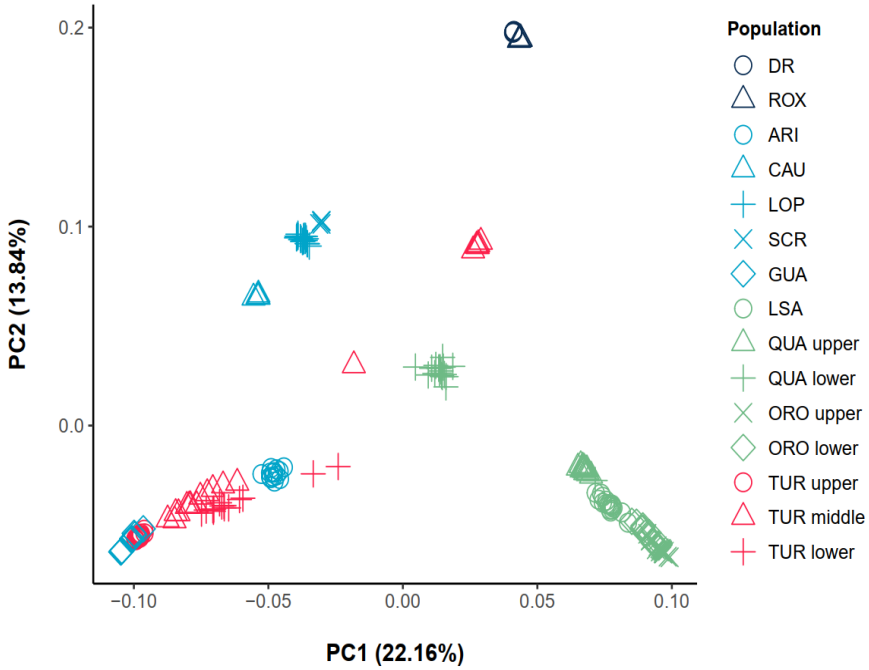

Figure 2. Principal Component Analysis of guppy populations based on genome-wide variation. Each point is one individual. Tobago, Caroni drainage, Oropouche drainage and Turure populations are coloured with dark blue, light blue, green and red, respectively.

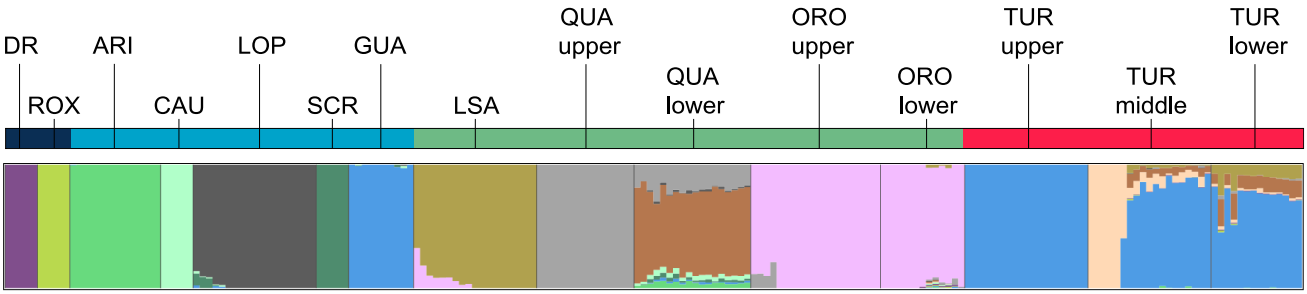

Figure 3. Admixture plots from analyses with optimal values of K (12). The regions are color-coded in the strip above the plots as follows: Tobago - dark blue, Caroni drainage - light blue, Oropouche drainage - green, and Turure - red.

Genome-wide nucleotide diversity estimates for 4-fold degenerated sites range from $2.3 \cdot 10^{-3}$ to $6.5 \cdot 10^{-3}$ per site, with the estimate for the upper Tururе site being similar to that for Guanapo source population ($3.22 \cdot 10^{-3}$ vs $2.67 \cdot 10^{-3}$, Fig. 4). Analyses of the lower sites in all rivers, but excluding the post-translocation Tururе populations, showed higher diversity in Oropouche than Caroni populations (estimate = -0.0022, se=0.0006, t= -2.899, p= 0.023) and Tobago (estimate = -0.0028, SE=0.0008, t= -3.495, p = 0.010).

To assess whether the translocated population exhibit signals of recent bottlenecks, we estimated Tajima's D values. Negative Tajima's D values indicates an excess of rare variants relative to neutral expectation under drift-mutation equilibrium. This can be caused by either recent population growth or by negative selection acting against mutations, while a positive Tajima's D indicating an excess of common variants suggests either balancing selection or a recent bottleneck that caused loss of rare variants. Our estimates based on 4-fold degenerated sites should thus reflect mostly demographic differences. Up-river sites showed significantly higher Tajima's D values than lower ones, and the upper Tururе had higher values than its source Guanapo population (Supplementary Fig. 1). However, the difference between Guanapo and the upper Tururre site was smaller than those of many

Oropouche populations, thus the allele frequency spectrum in this population suggesting only subtle effects of the translocation event.

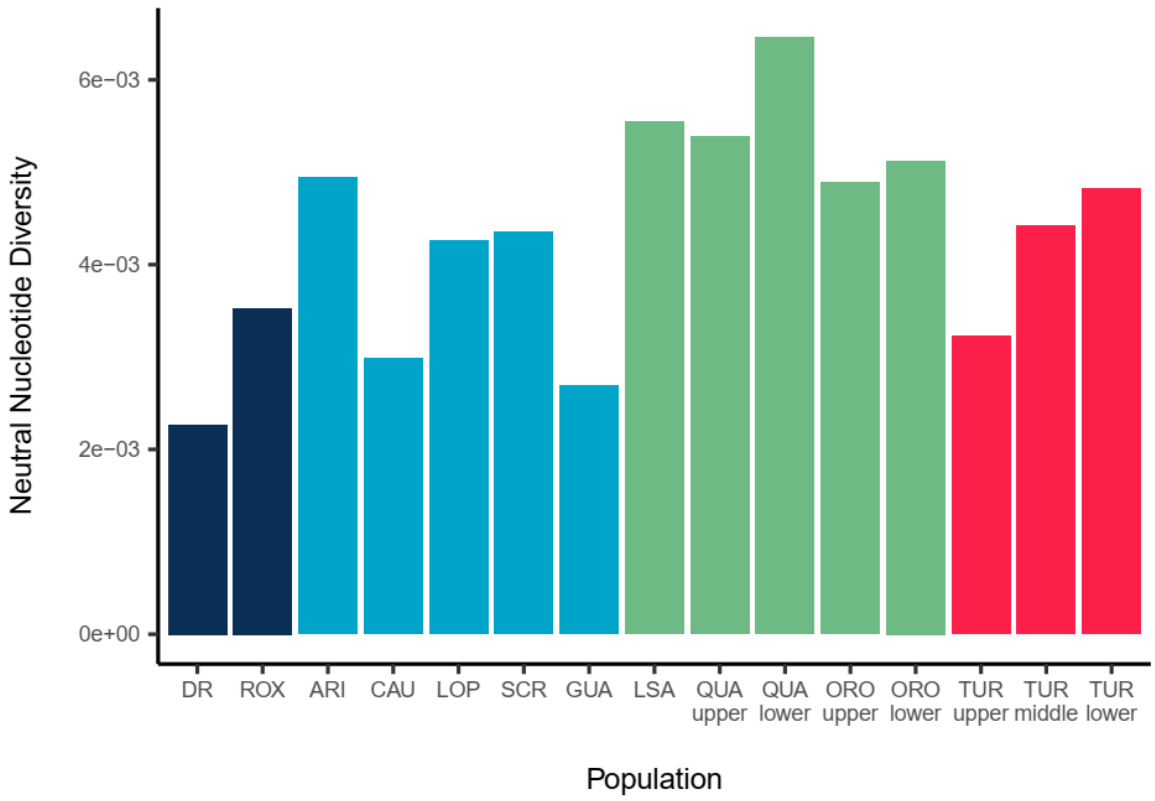

Figure 4. Nucleotide diversity estimates for 4-fold degenerated sites of the populations analysed. The regions are color-coded as follows: Tobago - dark blue, Caroni drainage - light blue, Oropouche drainage - green, and Tururе - red.

195 *2.2* ***Genetic load and its correlation with neutral diversity***

196 We calculated three measures of genetic load for each resequenced individual: *Relative Loss-of-*
197 *Function Load* (RLL), *Relative Genetic Load* (RGL) and *Relative Missense Load* (RML). The three
198 measures are expected to reflect the effects of different classes of deleterious mutations. As loss-of-
199 function (LoF) mutations are expected to be the most severe, with large expected effects on individual
200 fitness on average, thus we used RLL to reflects the effects of the most deleterious class of mutations.
201 The RGL estimate was based on conservation scores (CS) calculated from the observed number of
202 substitutions in multi-species alignment, relative to the number of expected substitutions under
203 neutrality (Davydov et al. 2010). This provides information on evolutionary constraints. Mutations
204 with high CS scores, have previously been utilized to estimate genetic load in many studies and are
205 already a well-established approach (Bertorelle et al. 2022) that probably includes effects of a wider
206 range of selection coefficients than LoF mutations. Finally, many missense mutations are weakly
207 deleterious and thus genetic load estimated based on these variants (RML) should reflect the least
208 deleterious classes of mutations.

209 To estimate genetic load, the guppy reference genome was first polarized using Illumina data from
210 two outgroup species, *X. maculatus* and *P. picta* (14x and 23x coverage, respectively). We inferred
211 ancestral states for the sites used for CS analyses; 42,860,381 sites (5.9% of the genome) yielded
212 information about both ancestral allele and CS. We called genotypes for these sites separately within
213 each guppy population. RGL value was then calculated per individual, as the sum of presumably
214 deleterious mutations (with CS>2) weighted by the CS value, relative to the value for all derived
215 variants. RLL and RML were respectively calculated as the ratio of loss-of-function (LoF) and
216 missense derived variant numbers to the number of derived synonymous variants in an individual's
217 genome. All three values (RGL, RLL and RML) were calculated separately for homozygous and
218 heterozygous genotypes, to reflect realized and masked genetic load, respectively. The sum of these
219 two to approximate total genetic load.

220 Genetic load differed among regions, with Oropouche populations generally having the lowest load,
221 significantly lower than Tobago in most comparisons (total RGL, realized RGL, total RML, realized
222 RML and masked RLL, Table S1) and lower than Caroni for total RGL (Supplementary Table 1).
223 Consequently, in models predicting genetic load from nucleotide diversity in a population after
224 accounting for regional differences we only found a significant negative association between
225 nucleotide diversity and total RGL (estimate = -2.451, SE=0.798, t= -3.069, P=0.022; Fig. 5), and the
226 region was not significant in any of these analyses. After removing the region we found that total
227 RGL and total RML were negatively associated with nucleotide diversity, whereas total RLL was not
228 significantly predicted by nucleotide diversity (Supplementary Table 2, Fig. 5). Nucleotide diversity
229 was also found to be negatively associated with masked RGL (Supplementary Table 2, Supplementary
230 Fig. 2).

For the two rivers with samples suitable for analysis, Oropouche and Quare, our comparisons of upstream versus downstream populations agreed with previous studies (Willing et al. 2010; Qiu et al. 2022), and generally support lower effective sizes and/or bottlenecks experienced during upstream colonization. As expected guppies from upstream sites tended to have higher load by almost all measures, except for masked RLL (Supplementary Table 3 and Supplementary Fig. 3).

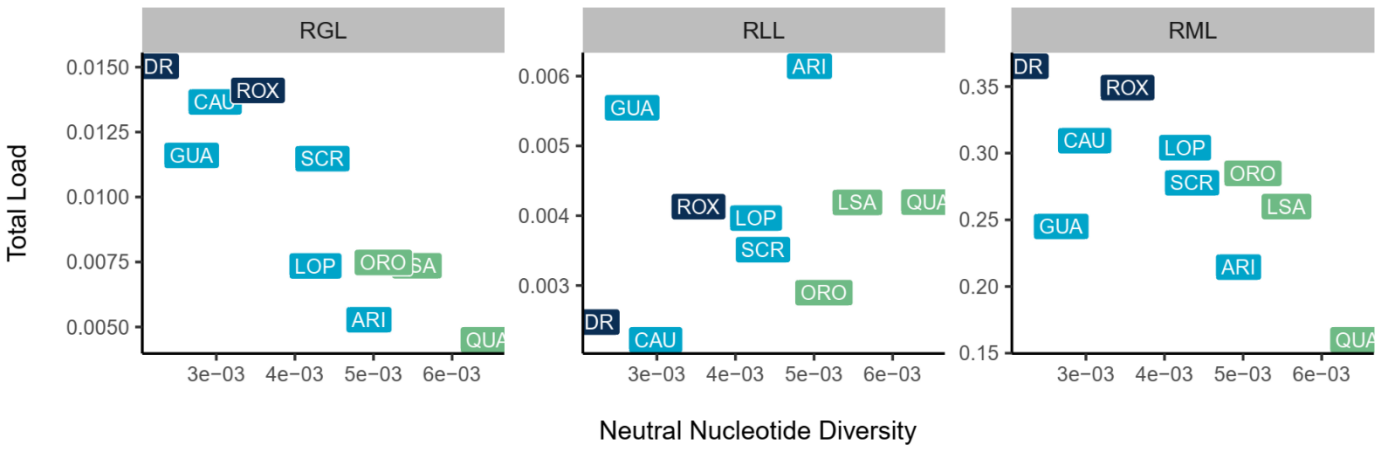

Figure 5. Relation between neutral nucleotide diversity (calculated in four-fold degenerated sites) and per-population estimates of relative genetic load averaged within populations.

236 *2.3* ***Genetic load in translocated and expanding population***

237 Comparison between the Guanapo (source) and upper Tururе (translocated) populations showed a
238 complex pattern of differences in genetic load (Supplementary Table 4, Fig. 6). The upper Tururе had
239 significantly lower values of total and masked RGL and RML, but higher realised RGL and RML
240 than the Guanapo. For RLL, however, the upper Tururе had significantly lower load for all three
241 measures than the Guanapo.

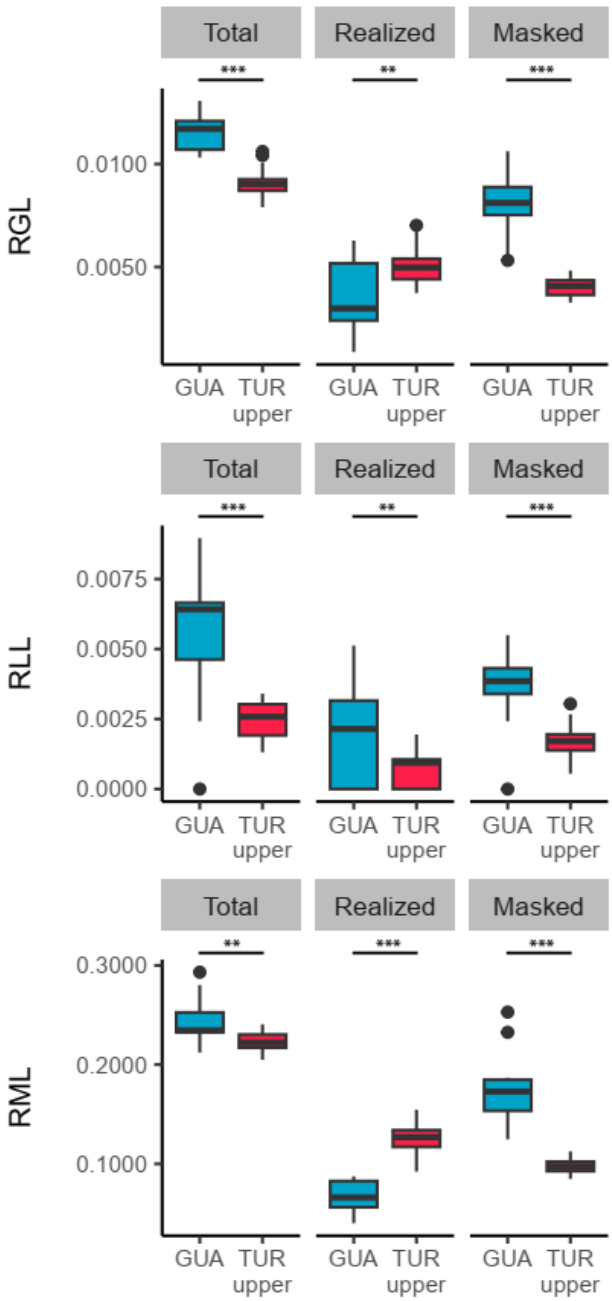

Figure 6. Comparisons of load estimates between Guanapo and upper Tururе – pre- and post-translocation populations respectively. Top panel represents relative genetic load (RGL), middle panel relative loss-of-function load (RLL) and bottom panel relative missense load (RML). Boxplots drawn from individual-based estimates and horizontal lines with asterisks indicate statistically significant differences.

Focusing on the three Turure populations, we found that upper Turure had significantly higher RGL and RML compared to downstream populations, except for masked RML and masked RGL, which did not differ significantly from those of lower Turure guppies (Supplementary Table 5, Fig. 7). Remarkably, the pattern was rev ersed for RLL: upper Turure had significantly lower total, masked and realised RLL compared to lower Turure, and also lower realized RLL compared to middle Turure (Supplementary Table 5, Fig. 7).

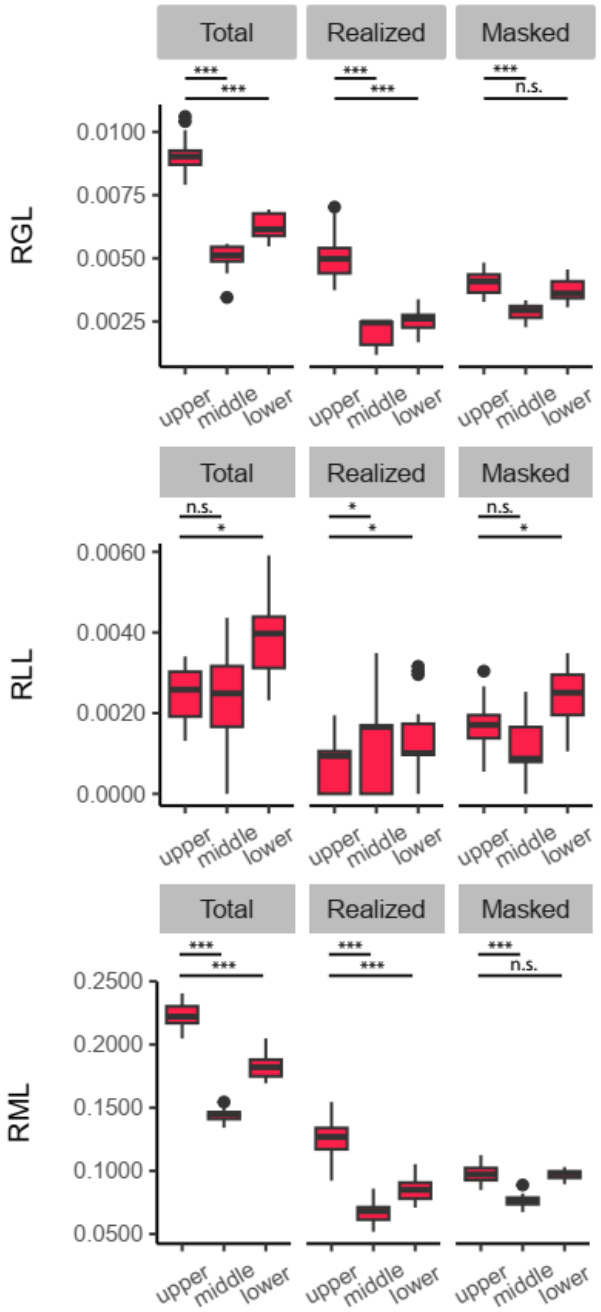

Figure 7. Comparisons of load estimates between the upper, middle and lower sites in Turure river. Top panel represents relative genetic load (RGL), middle panel relative loss-of-function load (RLL) and bottom panel relative missense load (RML). The boxplots were drawn using individual-based estimates and the horizontal lines with asterisks indicate statistically significant differences.

3. Discussion

The accelerating pace of global change, driven by climate shifts and habitat loss, has led to widespread species migration, range fragmentation, and population isolation (Johnson et al. 2017). These rapid demographic shifts can profoundly influence the dynamics of genetic load, creating challenges for conservation biology. To date, most research in this area has centered on endangered, highly vulnerable, or even extinct taxa (Kuang et al. 2020; Von Seth et al. 2021; Kleinman-Ruiz et al. 2022; Ochoa et al. 2022; Xie et al. 2022). The role of genetic load in biological invasions has received less attention (Tayeh et al. 2013; Rougemont et al. 2020; de Pedro et al. 2021). Our study addresses this gap by investigating how genetic load accumulates in invasive, non-threatened species (Lindholm et al. 2005; Deacon et al. 2011; Rosenthal et al. 2021), thereby offering insights into the mechanisms of invasion—particularly when accompanied by admixture with native populations. Our large population genomic dataset of hundreds of guppy genomes from multiple wild populations allowed us to show that genetic loads are strongly affected by historical effective population size (inferred from neutral diversity). We also found that translocated populations appear to have purged strongly deleterious mutations, and that subsequent admixture along the expansion gradient restored this load.

3.1. ***Genetic load correlates with historical effective population sizes***

Population genetics and conservation biology have long focused on how changes in population sizes shape the amount and distribution of deleterious variation (Bertorelle et al. 2022; van Oosterhout et al. 2022; Dussex et al. 2023; Robinson et al. 2023). Theoretical and empirical evidence suggest that prolonged reductions in effective population size, or bottlenecks lasting hundreds or thousands of generations, should allow weakly to moderately deleterious alleles to accumulate, although strongly deleterious alleles might also be purged (Xue et al. 2015; Robinson et al. 2018; Dussex et al. 2021; Mathur and DeWoody 2021; Kleinman-Ruiz et al. 2022). Therefore, long-term Ne (or neutral nucleotide diversity) should correlate with genetic load estimates within populations or species. Testing this predictions using inter-species comparisons has produced mixed results: although some studies reported the expected correlations (Schmidt et al. 2023; Wilder et al. 2023), another reported no correlation (Wooldridge et al. 2024). However, no consistent general framework exists for comparing genetic load across species (Teixeira and Huber 2021; Dussex et al. 2023). Further, endangered species - the typical focus of such work - rarely contain multiple populations with contrasting demographic histories and a broad range of effective population sizes. Intraspecific associations between Ne and genetic load have thus been studied in only a handful of cases (Mathur and DeWoody 2021; Kleinman-Ruiz et al. 2022; Mathur et al. 2023; Smeds et al. 2024). Our intraspecific analyses therefore provide valuable insight, showing that the expected negative relationship between neutral nucleotide diversity and relative genetic load is detectable—particularly when comparing a broad spectrum of mutation types, as estimated by RGL and RML.

3.2. ***Purging in translocated populations of invasive potential***

Our conclusion that the post-bottleneck Turure upper population experienced purging is based on the distinct patterns observed for RLL, the load reflecting the most strongly deleterious mutations, in comparison with load estimates based on wider ranges of mutation effects (RML and RGL). A population bottleneck alone is expected to increase the population's homozygote frequency, but not the expected frequency distribution of variants. Consequently, under increased genetic drift alone, realized load is predicted to increase while masked load declines, and total genetic load should remain

unchanged (García-Dorado 2012; Dussex et al. 2023). We detected the expected changes in masked and realized loads when comparing source and translocated populations' RML and RGL values (Fig. 6), though the total values have decreased slightly in the translocated populations, possibly due to selection purging the most deleterious variants in homozygous genotypes. As expected (Glémin 2003; Caballero et al. 2017; Dussex et al. 2023), the bottleneck effect is most pronounced for strongly deleterious mutations: all three classes of RLL (total, masked and realized) decreased following translocation. Similar effects on loads after bottlenecks have been documented in other species (Xue et al. 2015; Grossen et al. 2020; Khan et al. 2021; Ochoa and Gibbs 2021; Quinn et al. 2024; Stuart et al. 2025). Collectively, these findings provide strong evidence for purging (Dussex et al. 2023), suggesting that, under suitable conditions, highly deleterious mutations can be removed from bottlenecked populations, potentially increasing their invasiveness (Estoup et al. 2016). This has been proposed in the invasion of the harlequin ladybird (Facon et al. 2011) garlic mustard plant (Mullarkey et al. 2013) or bed bugs (Fountain et al. 2014). However, subsequent experimental evidence from the harlequin ladybird showed that bottlenecks had led to fixations of deleterious alleles more often than they purge them (Laugier et al. 2016), and transcriptomic analyses supported a tendency towards fixation, rather than purging of genetic load (Lombaert et al. 2025). Our analysis of translocated guppy populations does, however, provide clear evidence that purging occurred, as we detect changes in the type of genetic load, specifically by reduction of the most deleterious mutational class.

The Turure population that we infer to be purged of the most strongly deleterious mutations exhibits marked invasive potential, a possibility first raised when indigenous guppies were observed to be displaced (Shaw et al. 1992; Becher and Magurran 2000). Early genetic studies using allozymes confirmed that the translocated individuals established a viable population, overcame the natural waterfall barrier—likely aided by flooding events—and began spreading into different downstream environments (Shaw et al. 1992). Subsequent analyses of a panel of SNPs showed that fish from the middle reaches of the Turure clustered with the Caroni drainage (Willing et al. 2010), and more recent marker-based studies distinguishing local from invasive populations demonstrated that the invasion extended to, or beyond, the Turure–Quare confluence (Sievers et al. 2012). Continuous migration from above the barrier due to stochastic events such as flooding, together with subsequent effective mixing might explain this pattern (Sievers et al. 2012). However, the rapidity of the replacement of native fish in the downstream population, despite their larger effective population sizes, suggests that additional factors might have contributed to the success of the invaders. If so, Haskins' translocation experiment—designed to test the adaptive potential of guppies in novel environments—may ultimately have facilitated the loss of multiple populations within the drainage that were genetically distinct from guppies in other systems (Sievers et al. 2012).

The absence of strong geographic barriers in the lower Oropouche drainage likely promotes gene flow, which is particularly evident in the Quare population and, to a lesser extent, in La Seiva (Fig. 3). However, our analyses revealed no evidence of Turure ancestry in the lower Quare or La Seiva populations (Fig. 3), consistent with findings ~15 years earlier (Willing et al. 2010). Nonetheless, the Turure invasion proceeded rapidly, and our results suggest that the initial bottleneck—by increasing the efficiency of purging strongly deleterious mutations—may have contributed to this successful colonization. Other studies of bottlenecked vertebrate populations have yielded mixed conclusions ranging from no evidence of purging at all (Robinson et al. 2019; Ochoa et al. 2022; Smeds et al. 2024), purging of only the most deleterious class of mutations (Grossen et al. 2020; Khan et al. 2021;

Quinn et al. 2024), or accumulation of all classes of deleterious mutations (van der Valk et al. 2019). Disentangling whether such variation reflects methodological differences, limited statistical power, annotation quality, or true evolutionary processes remains difficult (Quinn et al. 2024). One critical factor may be the strength and duration of the bottleneck. Theory predicts that purging is most efficient under moderate reductions in population size, which expose recessive deleterious alleles to selection yet still allow selection to overcome genetic drift (Crow, 1970; Charlesworth et al., 1990; Glémin, 2003;Robinson et al., 2023; Lombaert et al. 2025). Consistent with this, Quinn et al. (2024), found evidence of purging of loss-of-function alleles in populations that experienced less severe size declines, whereas populations undergoing the most rapid and drastic bottlenecks showed weaker signals of purging. This pattern implies that extinction risk is the highest in severely reduced populations, where purging is the least effective. Our results align with these expectations. In the Turure river, the translocated population does not show a marked reduction in estimated neutral diversity or increase in Tajima's D values, compared with its progenitor (Fig. 4, Supplementary Fig. 4). This likely reflects the moderate severity of the bottleneck and the relatively large number of individuals introduced (see Introduction; (Shaw et al. 1992; Sievers et al. 2012)). Despite these subtle changes, we nevertheless detect pronounced shifts in the genetic load estimates, supporting the view that purging can be effective under moderate bottlenecks.

*3.3. **Admixture reshapes landscape of genetic load in expanding population***

Our investigation of the Turure expansion gradient revealed that total RGL and RML decline further downstream (Fig. 7), which could, in principle, reflect repeated purging events following successive bottlenecks. However, this should cause a gradual loss of nucleotide diversity and a depletion of rare variants, while purging should primarily reduce masked load by targeting the most deleterious mutations. In contrast, we found increased nucleotide diversity and lower Tajima's D values in the middle and lower Turure populations compared with the up-river population. Moreover, the decline in genetic load is driven mainly by reductions in realized load, whereas masked load remains largely unchanged or only moderately affected. Strikingly, for the most deleterious loss-of-function alleles, genetic load actually increases rather than decreases.

We therefore suggest that changes in genetic load down the Turure river primarily reflect admixture occurring below the waterfall barrier in the middle and lower reaches of the river. The upper and lower populations indeed differ substantially in their genetic composition, with the lower populations showing pronounced admixture with other ancestries (Fig. 3). Depending on the genetic makeup of the admixed sources and the degree of divergence between them, such admixture could have profoundly reshaped the landscape of genetic load by increasing the heterozygote frequencies and introducing new haplotypes into the population.

Our analyses revealed a strong correlation between total RGL and long-term effective population size, as inferred from neutral nucleotide diversity (Fig. 5). Rivers in the Oropouche drainage generally exhibit higher nucleotide diversity than those in the Caroni drainage (Fig. 4), suggesting that a lower total RGL should be expected in Oropouche populations. This pattern is also supported in our comparisons of total RGL between the two drainages (Supplementary Table 1). If the native Turure ancestry from the Oropouche drainage followed this trend, it would have carried fewer moderately deleterious mutations than the Caroni guppies introduced during translocation. Consequently, admixture between these ancestries should, on average, reduce the genetic load of the expanding population consistent with our observations. As expected, this reduction in total RGL (and similarly

in total RML) is driven primarily by decreases in realized load, likely reflecting the masking of moderately deleterious alleles that became fixed in the Caroni lineage after the Caroni-Oropouche divergence.

The most deleterious LoF mutations should rarely be fixed. Our neutral diversity dataset did not predict changes in RLL, suggesting that strongly deleterious mutations segregate and fix at comparable rates in different guppy populations (except for the purging in the Tururе up-river population explained above). We also detected no significant difference in RLL between the Oropouche and Caroni drainages (Fig. 5). Admixture is therefore the most likely explanation for an increase in RLL in the lower compared to upper Tururе, which likely counteracted purging by increasing heterozygosity, at the same time introducing new deleterious mutations from an unpurged native Tururе population (Fig. 8).

The influx of deleterious mutations through admixture depends on the relative demographic histories of the mixing populations which determine magnitude and patterns of expected change in genetic load. A well-studied example comes from anatomically modern human – Neanderthal hybridization (Harris and Nielsen 2016). Simulations shown that differences in effective population sizes could lead to a higher genetic load in the Neanderthal genomes, primarily due to differences in weakly deleterious mutations (based on estimates that the Neanderthal genome had approximately 1,000 more weakly deleterious mutations than anatomically modern human genomes). Gene flow from Neanderthals to anatomically modern humans after the Out of Africa expansion might therefore increase the recipient population's genetic load, prompting selection against Neanderthal ancestry. Empirical evidence supports this: Neanderthal alleles are underrepresented near coding and conserved sequences, and their overall ancestry decreases over time (Sankararaman et al. 2014; Juric et al. 2016). In contrast, in the expanding guppy population we studied, the admixed population initially had a higher relative genetic load than the native population with which it mixed, but carried fewer of the most highly deleterious mutations. The relative genetic load in the expanding population would therefore have decreased after admixture. Following the predictions outlined above, it would be interesting to investigate whether admixed ancestries in guppies are enriched in conserved sequences, opposite of the observation for Neanderthal ancestry in modern humans.

In a globally connected world, invasive species are recognized as one of the major threats to biodiversity, with effects on ecosystems that can be substantial and complex (Wallingford et al. 2020; Faulkner et al. 2024). Although biologists have long proposed that evolutionary processes may play a key role in invasion success (Estoup et al. 2016), it is only recently that the abundance of deleterious alleles has been considered. This is shaped by the accumulation of novel mutations over thousands of generations (van der Valk et al. 2019; Wootton et al. 2023), but these alleles can be rapidly redistributed through genetic drift, inbreeding, and gene flow. Our results demonstrate that invader populations can exhibit a reshaped landscape of genetic load, with both population size reductions and admixture exerting significant influence on these patterns.

*4. **Materials and methods***

*4.1 **Sampling and sequencing***

Individuals used in the study come from two batches of sampling and sequencing supplemented with 10 samples (Guanapo lower population) downloaded from European Nucleotide Archive BioProject PRJEB10680. First batch (51 individuals) of sampling took place in 2018 and was sequenced in 2019. Second batch (140 individuals) was both sampled and sequenced in 2022. All individuals are wild fish from natural populations in Trinidad and Tobago. The sampling procedures complied with the Polish law, European Directive 2010/63/EU and were conducted under permits issued by Ministry of Agriculture, Land and Fisheries of Trinidad and Tobago.

We sampled eight rivers on Trinidad - Aripo, Caura, Lopinot, and Santa Cruz (Caroni drainage), as well as La Seiva, Oropouche, Quare, Turure (Oropouche drainage) - and two rivers on Tobago: Dog River and Roxborough, collecting together 191 individuals from 14 sampling locations/populations in total. Three rivers were sampled at multiple sites: Quare (upper and lower), Oropouche (upper and lower), and Turure (upper, middle and lower); see Figure 1 and Supplementary Table 6 for more details and geographic coordinates. Fish were anesthetized using tricaine mesylate (MS-222) and preserved in 98% ethanol. Tail fin tissue was used for DNA extraction (with Thermo Scientific™ MagJET™ Genomic DNA kit) and genomic libraries generation (with the NEBNext® Ultra™ II FS DNA Library Prep Kit and NEBNext® Multiplex Oligos for Illumina® indices) according to manufacturer protocols. All samples were sequenced on Illumina NovaSeq 6000 platform using 2x150bp mode at the NGI Sweden. Together with downloaded from ENA archive Guanapo samples, 201 samples from 15 populations were included for subsequent analyses.

*4.2 **Population structure and nucleotide diversity***

Raw sequencing reads were filtered with Trimmomatic (version 0.39; (Bolger et al. 2014)) and aligned to guppy female reference genome (GCF_000633615.2; (Kunstner et al. 2016)) using bwa mem and default parameters (v0.7.10; (Li 2013)). Resulted BAM files were then subjected to duplicates marking with Picard tools (v2.21.6; http://broadinstitute.github.io/picard/). One sample from lower Oropouche yielded low mean coverage, so it was excluded from any further analyses leaving 200 samples in total.

To characterize the genetic composition of the samples, we performed principal component analysis (PCA) and ancestry inference. First, we jointly called variants in all BAM files using samtools mpileup (with -a AD parameter; v1.20, (Danecek et al. 2021)) and bcftools call (with -G populations indicating parameter and -m multiallelic parameter; v1.20) Resulting VCF was then filtered with bcftools (version 0.1.12b, (Danecek et al. 2011)) using the following thresholds: `MapppingQuality > 40, INFO/Depth < 5200, INFO/Depth > 1300, QUAL ≥ 30, MappingQualityBias > -3, ReadPositionBias < 3, SoftClipLengthBias < 3`; and with vcftools (v0.1.12b, Danecek et al. 2011): `MinorAlleleFraction ≥ 0.01, MaxAlelles = 2, MaxMissing = 50%; Depth ≥ 6 and GenotypeQuality ≥ 70`. We then used plink (v1.9; (Purcell et al. 2007)) to transform the VCF file into a BED file and prun it to avoid variants in linkage disequilibrium using 200bp window, 1bp step and 0.5 r^2 options. Resulting BED file was used to perform PCA. Using the same BED file, we ran Admixture (with -s random seed parameter; v1.3, (Alexander et al. 2009)) 10 times for each K

454 parameter (1-15). The Admixture results were plotted with pong software (with -s 0.95 threshold to
455 combine similar clusters at given K; v1.5, (Behr et al. 2016)).

456 In order to calculate neutral nucleotide diversity in our populations, we first identified fourfold-
457 degenerated sites in guppy genome using the find_4fds script (GitHub:
458 https://github.com/mattheatley/extract_4fds). We then called genotypes in our samples using the
459 same approach as above, but calling genotypes in both polymorphic and monomorphic sites.
460 Resulting VCF file was filtered with bcftools (v0.1.12b) as follows: `MapppingQuality > 40,`
461 `INFO/Depth < 5200, INFO/Depth > 1300, QUAL ≥ 30` and with vcftools (v0.1.12b): `MaxAlelles`
462 `= 2, MaxMissing = 50%; Depth ≥ 6 and` retained only those that were located in 4-fold
463 degenerated sites. Resulting files were used to calculate nucleotide diversity (π) in 1Mb windows
464 across the genome with pixy tool (v1.2.7.beta1; (Korunes and Samuk 2021)).

465 ### *4.3* ***Ancestral allele inference and Conservation Scores***

466 To infer guppy ancestral alleles (AA) we followed approach by Smeds et al. (2024) using genomic
467 information from two closely related outgroups: *Poecilia picta* and *Xiphophorus maculatus*.
468 Sequencing data for these two species was retrieved from NCBI's SRA (accession number
469 ERR4077394 and SRR13649980, respectively) in FASTQ format. Reads were mapped to the guppy
470 female reference genome and genotype calling was performed as described above, producing whole-
471 genome VCF files These files were then used in pseudo_haploidize.py script by Smeds et al. (2023,
472 GitHub: https://github.com/linneas/wolf-deleterious) to infer ancestral alleles based on allele depth
473 weight. Minimum depth thresholds were set to half of the expected coverage of *X. maculatus* and *P.*
474 *picta* (7 and 11 respectively), and the minimum genotype quality was set to 30. Haplotypes that did
475 not meet these thresholds were coded as "N". The two resulting BED files (one per species) were
476 merged and only sites where nucleotide was identical for both species (and not N) were retained as
477 informative for ancestral allele inference.

478 To obtain conservation scores (CS), we downloaded CS BED file from the Ensembl fish Compara
479 database (release 111, 65 fish species alignment, CS calculated with GERP, (Herrero et al. 2016)).
480 The file was intersected with the ancestral allele BED file. The resulting CS-AA BED was used for
481 genotype filtering, as described below.

482 ### *4.4* ***Genetic Load estimation***

483 To estimate genetic load, we developed a bioinformatic pipeline analyzing within population genomic
484 variation. Each population was analyzed separately, allowing for parallelization and detection of rare
485 variants. First, we inferred genotypes with GATK HaplotypeCaller (with `-ERC BP_RESOLUTION` and
486 `--output-mode EMIT_ALL_CONFIDENT_SITES` parameters, v4.1.4.1; (McKenna et al. 2010)). Single
487 individual genomic VCF files (GVFCs) were merged into population GVCFs (GATK
488 CombineGVCFs) and used in GATK GenotypeGVCFs to produce VCF files in all sites mode (`-all-`
489 `sites`). Sites with fewer than 70% of genotypes meeting quality thresholds (DP ≥ 6 and GQ ≥ 30)
490 were removed. Subsequently, we filtered out multiallelic sites and kept only sites that had both CS
491 and AA as one of the two alleles. Information about CS and AA were added to the INFO field using
492 custom Python script. In case of sites, where AA was the alternative to the reference nucleotide, the
493 two alleles were swapped, so that REF always represents ancestral allele in the final VCF file.

Because our samples differed in expected coverage, we applied individual-depth-based filtering. Only genotypes meeting the criteria 2 × mean DP of the individual ≥ DP ≥ 6 and GQ ≥ 30 were retained; genotypes failing these thresholds were coded as missing. Sites with more than 30% missing genotypes were excluded. Finally we extracted SNPs and removed variants failing GATK-recommended quality filters: (`QualityByDepth ≥ 2, MappingQuality ≥ 40, FisherScore ≤ 60, StrandOddsRatio ≤ 3, MappingQualityRankSum ≥ -12.5, ReadPosRankSum ≥ -8`).

Per-individual relative genetic load (RGL) was calculated following the approach of Dussex et al. (2021), using the following formula:

$$RGL = \frac{\sum_{\substack{i=1 \\ CS_i \geq 2}}^{n} CS_i \cdot D_i}{\sum_{i=1}^{n} D_i}$$

where n is the number of variants, CS_i is the conservation score and D_i is the number of derived alleles of the ith variant. Only alleles at highly conserved sites (conservation score ≥ 2) were included in the numerator.

Additionally, we used called SNPs to identify loss of function (LOF, nonsense), missense and synonymous variants with SNPEff tool (v5.0; (Cingolani et al. 2012)). The values were calculated and normalized against synonymous derived alleles to calculate relative LOF load (RLL) using following formulas:

$$RLL = \frac{\sum_{\substack{i=1 \\ t \in LOF}}^{n} D_i}{\sum_{\substack{i=1 \\ t \in syn}}^{n} D_i}$$

where n is the number of variants, t is the variant type and D_i is the number of derived alleles of the ith variant.

Similarly, values for missense alleles were also used to calculate relative missense load (RML) using the following formula:

$$RML = \frac{\sum_{\substack{i=1 \\ t \in mis}}^{n} D_i}{\sum_{\substack{i=1 \\ t \in syn}}^{n} D_i}$$

where n is the number of variants, t is the variant type and D_i is the number of derived alleles of the ith variant.

The calculations were done separately for all variants (as a proxy for total genetic load), heterozygous genotypes (masked genetic load) and homozygous genotypes (realized genetic load).

4.5. ***Statistical analyses***

All statistical analyses were performed in R (v4.5.0) Model assumptions were verified by examining diagnostic plots of residuals (or simulated residuals where appropriate) using DHARMa package (Hartig 2016).

The association between mutation load and nucleotide diversity, was tested using general or generalized linear models, with gaussian distribution for RGL, and binomial for RML and RLL. Logarithmic transformation was used to deal with detected heteroschedascidity (reported in Table S1). We initially fitted region in this models along with population, but region was not significant in any analysis and some models containing it did not conform to model assumptions (heteroscedasticity), which improved when Region was removed, Therefore, we focused our analyses on the models without the region.

Comparison of genetic load between regions was done using general or generalized mixed models using glmmTMB package, with population entered as a random effect. Gaussian distribution was modelled for RGL, and binomial for RML and RLL. Comparisons between populations within Turure, between Turure and Guanapo and between upper and lower parts of streams within Oropuche was analyzed with general (RGL) or generalized (RGL and RLL) linear models. For generalized models, we used binomial distribution, or, when over or under dispersion was detected, quasibinomial distribution (in which case we report dispersion parameter, Tables S3 – S5).

In analysis of islands and relation with Ne, only the lower river sites were used. Additionally, in tests regarding effective population size correlation, islands and sites comparisons, all Turure populations were excluded due to their atypical characteristics (recent bottleneck, expansion and hybridization).

Acknowledgements

We are grateful to Deborah Charlesworth, Wiesław Babik and Jonathan Parrett for their valuable comments on an early version of the manuscript, and to the members of the Evolutionary Biology Group for their insightful discussions and continuous support. This work was funded by the Polish National Science Centre 2018/31/D/NZ8/00091 grant. M.K. was supported by the Polish National Agency for Academic Exchange under Bekker Programme. Computations were performed at the Poznan Supercomputing and Networking Centre. We are also grateful to the Fisheries Division of Ministry of Agriculture, Land and Fisheries, Republic of Trinidad and Tobago for granting permission for collecting and export of fish tissue.

Data Availability

Individual sample resequencing data are available from NCBI under Bioproject PRJNA1040274. Guanapo population samples were downloaded from ENA Bioproject PRJEB10680. *P. picata* and *X. maculatus* samples were downloaded from NCBI Bioprojects ERR4077394 and SRR13649980. Scripts used in this work are available on GitHub: https://github.com/0-Ioniel-0/Expansion_Load.

*5. **References***

Alexander DH, Novembre J, Lange K. 2009. Fast model-based estimation of ancestry in unrelated individuals. Genome Res. 19:1655–1664.

Barker BS, Cocio JE, Anderson SR, Braasch JE, Cang FA, Gillette HD, Dlugosch KM. 2019. Potential limits to the benefits of admixture during biological invasion. Mol. Ecol. 28:100–

113.
Barrett SCH, Charlesworth D. 1991. Effects of a change in the level of inbreeding on the genetic load. Nature 352:522–524.
Bassar RD, Marshall MC, López-Sepulcre A, Zandonà E, Auer SK, Travis J, Pringle CM, Flecker AS, Thomas SA, Fraser DF. 2010. Local adaptation in Trinidadian guppies alters ecosystem processes. Proc. Natl. Acad. Sci. 107:3616–3621.
Becher SA, Magurran AE. 2000. Gene flow in Trinidadian guppies. J. Fish Biol. 56:241–249.
Behr AA, Liu KZ, Liu-Fang G, Nakka P, Ramachandran S. 2016. Pong: fast analysis and visualization of latent clusters in population genetic data. Bioinformatics 32:2817–2823.
Bertorelle G, Raffini F, Bosse M, Bortoluzzi C, Iannucci A, Trucchi E, Morales HE, van Oosterhout C. 2022. Genetic load: genomic estimates and applications in non-model animals. Nat. Rev. Genet. 23:492–503.
Bolger AM, Lohse M, Usadel B. 2014. Trimmomatic: A flexible trimmer for Illumina sequence data. Bioinformatics 30:2114–2120.
Caballero A, Bravo I, Wang J. 2017. Inbreeding load and purging: implications for the short-term survival and the conservation management of small populations. Heredity (Edinb). 118:177–185.
Charlesworth D, Willis JH. 2009. The genetics of inbreeding depression. Nat. Rev. Genet.
Cingolani P, Platts A, Wang LL, Coon M, Nguyen T, Wang L, Land SJ, Lu X, Ruden DM. 2012. A program for annotating and predicting the effects of single nucleotide polymorphisms, SnpEff: SNPs in the genome of Drosophila melanogaster strain w1118; iso-2; iso-3. Fly (Austin). 6:80–92.
Colautti RI, Alexander JM, Dlugosch KM, Keller SR, Sultan SE. 2017. Invasions and extinctions through the looking glass of evolutionary ecology. Philos. Trans. R. Soc. B Biol. Sci. 372:20160031.
Crnokrak P, Barrett SCH. 2002. Perspective: purging the genetic load: a review of the experimental evidence. Evolution (N. Y). 56:2347–2358.
Crow JF. 1989. Some possibilities for measuring selection intensities in man. Hum. Biol. 61:763–775.
Danecek P, Auton A, Abecasis G, Albers CA, Banks E, DePristo MA, Handsaker RE, Lunter G, Marth GT, Sherry ST, et al. 2011. The variant call format and VCFtools. Bioinformatics 27:2156–2158.
Danecek P, Bonfield JK, Liddle J, Marshall J, Ohan V, Pollard MO, Whitwham A, Keane T, McCarthy SA, Davies RM. 2021. Twelve years of SAMtools and BCFtools. Gigascience 10:giab008.
Davydov E V, Goode DL, Sirota M, Cooper GM, Sidow A, Batzoglou S. 2010. Identifying a high fraction of the human genome to be under selective constraint using GERP++. PLoS Comput. Biol. 6:e1001025.
Deacon AE, Ramnarine IW, Magurran AE. 2011. How reproductive ecology contributes to the spread of a globally invasive fish. PLoS One 6:e24416.
Dehasque M, Morales HE, Díez-del-Molino D, Pečnerová P, Chacón-Duque JC, Kanellidou F, Muller H, Plotnikov V, Protopopov A, Tikhonov A. 2023. Temporal dynamics of woolly mammoth genome erosion prior to extinction. Cell.
Devigili A, Fitzpatrick JL, Gasparini C, Ramnarine IW, Pilastro A, Evans JP. 2018. Possible glimpses into early speciation: The effect of ovarian fluid on sperm velocity accords with post-copulatory isolation between two guppy populations. J. Evol. Biol. 31:66–74.
Dussex N, Morales HE, Grossen C, Dalén L, van Oosterhout C. 2023. Purging and accumulation of genetic load in conservation. Trends Ecol. Evol.
Dussex N, Van Der Valk T, Morales HE, Wheat CW, Díez-del-Molino D, Von Seth J, Foster Y, Kutschera VE, Guschanski K, Rhie A. 2021. Population genomics of the critically endangered kākāpō. Cell Genomics 1.
Endler JA. 1980. Natural Selection on Color Patterns in Poecilia reticulata. Evolution (N. Y).

Estoup A, Ravigné V, Hufbauer R, Vitalis R, Gautier M, Facon B. 2016. Is there a genetic paradox of biological invasion? Annu. Rev. Ecol. Evol. Syst. 47:51–72.
Eyre-Walker A, Keightley PD. 2007. The distribution of fitness effects of new mutations. Nat. Rev. Genet. 8:610–618.
Facon B, Hufbauer RA, Tayeh A, Loiseau A, Lombaert E, Vitalis R, Guillemaud T, Lundgren JG, Estoup A. 2011. Inbreeding depression is purged in the invasive insect Harmonia axyridis. Curr. Biol. 21:424–427.
Fajen A, Breden F. 1992. Mitochondrial DNA sequence variation among natural populations of the Trinidad guppy, Poecilia reticulata. Evolution (N. Y). 46:1457–1465.
Faulkner KT, Hulme PE, Wilson JRU. 2024. Harder, better, faster, stronger? Dispersal in the Anthropocene. Trends Ecol. Evol. 39:1130–1140.
Fitzpatrick SW, Gerberich JC, Angeloni LM, Bailey LL, Broder ED, Torres-Dowdall J, Handelsman CA, López-Sepulcre A, Reznick DN, Ghalambor CK. 2016. Gene flow from an adaptively divergent source causes rescue through genetic and demographic factors in two wild populations of T rinidadian guppies. Evol. Appl. 9:879–891.
Fountain T, Duvaux L, Horsburgh G, Reinhardt K, Butlin RK. 2014. Human-facilitated metapopulation dynamics in an emerging pest species, C imex lectularius. Mol. Ecol. 23:1071–1084.
Fraser BA, Künstner A, Reznick DN, Dreyer C, Weigel D. 2015. Population genomics of natural and experimental populations of guppies (Poecilia reticulata). Mol. Ecol.
García-Dorado A. 2012. Understanding and predicting the fitness decline of shrunk populations: inbreeding, purging, mutation, and standard selection. Genetics 190:1461–1476.
Glémin S. 2003. How are deleterious mutations purged? Drift versus nonrandom mating. Evolution (N. Y). 57:2678–2687.
Grossen C, Guillaume F, Keller LF, Croll D. 2020. Purging of highly deleterious mutations through severe bottlenecks in Alpine ibex. Nat. Commun. 11:1001.
Harris K, Nielsen R. 2016. The genetic cost of Neanderthal introgression. Genetics 203:881–891.
Hartig F. 2016. DHARMa: residual diagnostics for hierarchical (multi-level/mixed) regression models. CRAN Contrib. Packag.
Herrero J, Muffato M, Beal K, Fitzgerald S, Gordon L, Pignatelli M, Vilella AJ, Searle SMJ, Amode R, Brent S. 2016. Ensembl comparative genomics resources. Database 2016:bav096.
Johnson CN, Balmford A, Brook BW, Buettel JC, Galetti M, Guangchun L, Wilmshurst JM. 2017. Biodiversity losses and conservation responses in the Anthropocene. Science (80-.). 356:270–275.
Juric I, Aeschbacher S, Coop G. 2016. The strength of selection against Neanderthal introgression. PLoS Genet. 12:e1006340.
Kardos M, Armstrong EE, Fitzpatrick SW, Hauser S, Hedrick PW, Miller JM, Tallmon DA, Funk WC. 2021. The crucial role of genome-wide genetic variation in conservation. Proc. Natl. Acad. Sci. 118:e2104642118.
Kardos M, Zhang Y, Parsons KM, Kang H, Xu X, Liu X, Matkin CO, Zhang P, Ward EJ, Hanson MB. 2023. Inbreeding depression explains killer whale population dynamics. Nat. Ecol. Evol. 7:675–686.
Keller LF, Waller DM. 2002. Inbreeding effects in wild populations. Trends Ecol. Evol. 17:230–241.
Kemp DJ, Batistic F-K, Reznick DN. 2018. Predictable adaptive trajectories of sexual coloration in the wild: evidence from replicate experimental guppy populations. Evolution (N. Y). 72:2462–2477.
Khan A, Patel K, Shukla H, Viswanathan A, van der Valk T, Borthakur U, Nigam P, Zachariah A, Jhala Y V, Kardos M. 2021. Genomic evidence for inbreeding depression and purging of deleterious genetic variation in Indian tigers. Proc. Natl. Acad. Sci. 118:e2023018118.
Kimura M, Maruyama T, Crow JF. 1963. THE MUTATION LOAD IN SMALL POPULATIONS. Genetics.

Kimura M, Ohta T. 1969. The average number of generations until fixation of a mutant gene in a finite population. Genetics 61:763.
Kleinman-Ruiz D, Lucena-Perez M, Villanueva B, Fernández J, Saveljev AP, Ratkiewicz M, Schmidt K, Galtier N, García-Dorado A, Godoy JA. 2022. Purging of deleterious burden in the endangered Iberian lynx. Proc. Natl. Acad. Sci. 119:e2110614119.
Kołodziejczyk J, Fijarczyk A, Porth I, Robakowski P, Vella N, Vella A, Kloch A, Biedrzycka A. 2025. Genomic investigations of successful invasions: the picture emerging from recent studies. Biol. Rev.
Korunes KL, Samuk K. 2021. pixy: Unbiased estimation of nucleotide diversity and divergence in the presence of missing data. Mol. Ecol. Resour. 21:1359–1368.
Kuang W, Hu J, Wu H, Fen X, Dai Q, Fu Q, Xiao W, Frantz L, Roos C, Nadler T. 2020. Genetic diversity, inbreeding level, and genetic load in endangered snub-nosed monkeys (Rhinopithecus). Front. Genet. 11:615926.
Kunstner A, Hoffmann M, Fraser BA, Kottler VA, Sharma E, Weigel D, Dreyer C. 2016. The genome of the trinidadian guppy, Poecilia reticulata, and variation in the Guanapo population. PLoS One 11:e0169087.
Kyriazis CC, Wayne RK, Lohmueller KE. 2021. Strongly deleterious mutations are a primary determinant of extinction risk due to inbreeding depression. Evol. Lett. [Internet] 5:33–47. Available from: https://onlinelibrary.wiley.com/doi/full/10.1002/evl3.209
Lan T, Li H, Liu B, Shi M, Tian Y, Sahu SK, Cui L, Dussex N, Liu D, Ma Y. 2025. Revealing extensive inbreeding and less efficient purging of deleterious mutations in wild Amur tigers in China. J. Genet. Genomics 52:641–649.
Laugier GJM, Le Moguédec G, Su W, Tayeh A, Soldati L, Serrate B, Estoup A, Facon B. 2016. Reduced population size can induce quick evolution of inbreeding depression in the invasive ladybird Harmonia axyridis. Biol. Invasions 18:2871–2881.
Li H. 2013. Aligning sequence reads, clone sequences and assembly contigs with BWA-MEM. arXiv Prepr. arXiv [Internet] 00:3. Available from: http://arxiv.org/abs/1303.3997
Lindholm AK, Breden F, Alexander HJ, CHAN W, Thakurta SG, Brooks R. 2005. Invasion success and genetic diversity of introduced populations of guppies Poecilia reticulata in Australia. Mol. Ecol. 14:3671–3682.
Lombaert E, Blin A, Porro B, Guillemaud T, Bernal JS, Chang G, Kirichenko N, Sappington TW, Toepfer S, Deleury E. 2025. Unraveling genetic load dynamics during biological invasion: insights from two invasive insect species. Peer Community J. 5.
Lynch M, Conery J, Burger R, Lande R. 1995. Mutation accumulation and the extinction of small populations. Science (80-.). 146:1455–1460.
Magurran AE. 2005. Evolutionary ecology: the Trinidadian guppy.
Mathur S, DeWoody JA. 2021. Genetic load has potential in large populations but is realized in small inbred populations. Evol. Appl. 14:1540–1557.
Mathur S, Mason AJ, Bradburd GS, Gibbs HL. 2023. Functional genomic diversity is correlated with neutral genomic diversity in populations of an endangered rattlesnake. Proc. Natl. Acad. Sci. 120:e2303043120.
McKenna A, Hanna M, Banks E, Sivachenko A, Cibulskis K, Kernytsky A, Garimella K, Altshuler D, Gabriel S, Daly M, et al. 2010. The Genome Analysis Toolkit: A MapReduce framework for analyzing next-generation DNA sequencing data. Genome Res. 20:1297–1303.
Mullarkey AA, Byers DL, Anderson RC. 2013. Inbreeding depression and partitioning of genetic load in the invasive biennial Alliaria petiolata (Brassicaceae). Am. J. Bot. 100:509–518.
Ochoa A, Gibbs HL. 2021. Genomic signatures of inbreeding and mutation load in a threatened rattlesnake. Mol. Ecol. 30:5454–5469.
Ochoa A, Onorato DP, Roelke-Parker ME, Culver M, Fitak RR. 2022. Give and take: Effects of genetic admixture on mutation load in endangered Florida panthers. J. Hered. 113:491–499.
van Oosterhout C, Speak SA, Birley T, Bortoluzzi C, Percival-Alwyn L, Urban LH, Groombridge JJ, Segelbacher G, Morales HE. 2022. Genomic erosion in the assessment of species extinction

risk and recovery potential. BioRxiv:2009–2022.
de Pedro M, Riba M, González-Martínez SC, Seoane P, Bautista R, Claros MG, Mayol M. 2021. Demography, genetic diversity and expansion load in the colonizing species Leontodon longirostris (Asteraceae) throughout its native range. Mol. Ecol. 30:1190–1205.
Peischl S, Kirkpatrick M, Excoffier L. 2015. Expansion load and the evolutionary dynamics of a species range. Am. Nat. 185:E81–E93.
Purcell S, Neale B, Todd-Brown K, Thomas L, Ferreira MAR, Bender D, Maller J, Sklar P, de Bakker PIW, Daly MJ, et al. 2007. PLINK: a tool set for whole-genome association and population-based linkage analyses. Am. J. Hum. Genet. 81:559–575.
Qiu S, Yong L, Wilson A, Croft DP, Graham C, Charlesworth D. 2022. Partial sex linkage and linkage disequilibrium on the guppy sex chromosome. Mol. Ecol. 31:5524–5537.
Quinn CB, Preckler-Quisquater S, Buchalski MR, Sacks BN. 2024. Whole genomes inform genetic rescue strategy for montane red foxes in North America. Mol. Biol. Evol. 41:msae193.
Ralls K, Sunnucks P, Lacy RC, Frankham R. 2020. Genetic rescue: A critique of the evidence supports maximizing genetic diversity rather than minimizing the introduction of putatively harmful genetic variation. Biol. Conserv. 251.
Reznick DA, Bryga H, Endler JA. 1990. Experimentally induced life-history evolution in a natural population. Nature 346:357–359.
Reznick DN, Bryga H. 1987. Life-history evolution in guppies (Poecilia reticulata): 1. Phenotypic and genetic changes in an introduction experiment. Evolution (N. Y). 41:1370–1385.
Robinson J, Kyriazis CC, Yuan SC, Lohmueller KE. 2023. Deleterious variation in natural populations and implications for conservation genetics. Annu. Rev. Anim. Biosci. 11:93–114.
Robinson JA, Brown C, Kim BY, Lohmueller KE, Wayne RK. 2018. Purging of strongly deleterious mutations explains long-term persistence and absence of inbreeding depression in island foxes. Curr. Biol. 28:3487–3494.
Robinson JA, Ortega-Del Vecchyo D, Fan Z, Kim BY, Marsden CD, Lohmueller KE, Wayne RK. 2016. Genomic flatlining in the endangered island fox. Curr. Biol. 26:1183–1189.
Robinson JA, Räikkönen J, Vucetich LM, Vucetich JA, Peterson RO, Lohmueller KE, Wayne1 RK. 2019. Genomic signatures of extensive inbreeding in Isle Royale wolves, a population on the threshold of extinction. Sci. Adv. 5.
Rosenthal WC, McIntyre PB, Lisi PJ, Prather Jr RB, Moody KN, Blum MJ, Hogan JD, Schoville SD. 2021. Invasion and rapid adaptation of guppies (Poecilia reticulata) across the Hawaiian Archipelago. Evol. Appl. 14:1747–1761.
Rougemont Q, Leroy T, Rondeau EB, Koop B, Bernatchez L. 2023. Allele surfing causes maladaptation in a Pacific salmon of conservation concern. PLoS Genet. 19:e1010918.
Rougemont Q, Moore JS, Leroy T, Normandeau E, Rondeau EB, Withler RE, van Doornik DM, Crane PA, Naish KA, Garza JC, et al. 2020. Demographic history shaped geographical patterns of deleterious mutation load in a broadly distributed Pacific Salmon. PLoS Genet. 16.
Russell ST, Magurran AE. 2006. Intrinsic reproductive isolation between Trinidadian populations of the guppy, Poecilia reticulata. J. Evol. Biol. 19:1294–1303.
Sankararaman S, Mallick S, Dannemann M, Prüfer K, Kelso J, Pääbo S, Patterson N, Reich D. 2014. The genomic landscape of Neanderthal ancestry in present-day humans. Nature 507:354–357.
Schmidt C, Hoban S, Hunter M, Paz-Vinas I, Garroway CJ. 2023. Genetic diversity and IUCN Red List status. Conserv. Biol. 37:e14064.
Schories S, Meyer MK, Schartl M. 2009. Description of Poecilia (Acanthophacelus) obscura n. sp.,(Teleostei: Poeciliidae), a new guppy species from western Trinidad, with remarks on P. wingei and the status of the Endler s guppy. Zootaxa 2266:35–50.
Von Seth J, Dussex N, Díez-del-Molino D, Van Der Valk T, Kutschera VE, Kierczak M, Steiner CC, Liu S, Gilbert MTP, Sinding M-HS. 2021. Genomic insights into the conservation status of the world's last remaining Sumatran rhinoceros populations. Nat. Commun. 12:2393.
Shaw PW, Carvalho GR, Seghers BH, Magurran AE. 1992. Genetic consequences of an artificial

introduction of guppies (Poecilia reticulata) in N Trinidad. Proc. - R. Soc. London, B.
Sievers C, Willing E-M, Hoffmann M, Dreyer C, Ramnarine I, Magurran A. 2012. Reasons for the invasive success of a guppy (Poecilia reticulata) population in Trinidad. PLoS One 7:e38404.
Smeds L, Huson LSA, Ellegren H. 2024. Structural genomic variation in the inbred Scandinavian wolf population contributes to the realized genetic load but is positively affected by immigration. Evol. Appl. 17:e13652.
Stewart GS, Morris MR, Genis AB, Szűcs M, Melbourne BA, Tavener SJ, Hufbauer RA. 2017. The power of evolutionary rescue is constrained by genetic load. Evol. Appl. 10:731–741.
Stuart OP, Cleave R, Pearce K, Magrath MJL, Mikheyev AS. 2025. Purging of highly deleterious mutations through an extreme bottleneck. Mol. Biol. Evol. 42:msaf079.
Tayeh A, Estoup A, Hufbauer RA, Ravigné V, Goryacheva I, Zakharov IA, Lombaert E, Facon B. 2013. Investigating the genetic load of an emblematic invasive species: the case of the invasive harlequin ladybird Harmonia axyridis. Ecol. Evol. 3:864–871.
Teixeira JC, Huber CD. 2021. The inflated significance of neutral genetic diversity in conservation genetics. Proc. Natl. Acad. Sci. U. S. A. 118.
van der Valk T, Díez-del-Molino D, Marques-Bonet T, Guschanski K, Dalén L. 2019. Historical Genomes Reveal the Genomic Consequences of Recent Population Decline in Eastern Gorillas. Curr. Biol. 29:165-170.e6.
Wagner NK, Ochocki BM, Crawford KM, Compagnoni A, Miller TEX. 2017. Genetic mixture of multiple source populations accelerates invasive range expansion. J. Anim. Ecol. 86:21–34.
Wallingford PD, Morelli TL, Allen JM, Beaury EM, Blumenthal DM, Bradley BA, Dukes JS, Early R, Fusco EJ, Goldberg DE. 2020. Adjusting the lens of invasion biology to focus on the impacts of climate-driven range shifts. Nat. Clim. Chang. 10:398–405.
Whiting JR, Paris JR, van der Zee MJ, Parsons PJ, Weigel D, Fraser BA. 2021. Drainage-structuring of ancestral variation and a common functional pathway shape limited genomic convergence in natural high- And low-predation guppies. PLoS Genet. 17:1–29.
Wilder AP, Supple MA, Subramanian A, Mudide A, Swofford R, Serres-Armero A, Steiner C, Koepfli K-P, Genereux DP, Karlsson EK. 2023. The contribution of historical processes to contemporary extinction risk in placental mammals. Science (80-.). 380:eabn5856.
Willing EM, Bentzen P, Van Oosterhout C, Hoffmann M, Cable J, Breden F, Weigel D, Dreyer C. 2010. Genome-wide single nucleotide polymorphisms reveal population history and adaptive divergence in wild guppies. Mol. Ecol.
Wooldridge B, Orland C, Enbody E, Escalona M, Mirchandani C, Corbett-Detig R, Kapp JD, Fletcher N, Cox-Ammann K, Raimondi P. 2024. Limited genomic signatures of population collapse in the critically endangered black abalone (Haliotis cracherodii). Mol. Ecol.:e17362.
Wootton E, Robert C, Taillon J, Côté SD, Shafer ABA. 2023. Genomic health is dependent on long-term population demographic history. Mol. Ecol. 32:1943–1954.
Wright S. 1922. Coefficients of inbreeding and relationship. Am. Nat. 56:330–338.
Wright S. 1932. The roles of mutation, inbreeding, crossbreeding, and selection in evolution.
Xie H-X, Liang X-X, Chen Z-Q, Li W-M, Mi C-R, Li M, Wu Z-J, Zhou X-M, Du W-G. 2022. Ancient demographics determine the effectiveness of genetic purging in endangered lizards. Mol. Biol. Evol. 39:msab359.
Xue Y, Prado-Martinez J, Sudmant PH, Narasimhan V, Ayub Q, Szpak M, Frandsen P, Chen Y, Yngvadottir B, Cooper DN. 2015. Mountain gorilla genomes reveal the impact of long-term population decline and inbreeding. Science (80-.). 348:242–245.
Zayed A, Constantin ŞA, Packer L. 2007. Successful biological invasion despite a severe genetic load. PLoS One 2:e868.
Zeitler L, Parisod C, Gilbert KJ. 2023. Purging due to self-fertilization does not prevent accumulation of expansion load. PLoS Genet. 19:e1010883.

Supplementary Figures

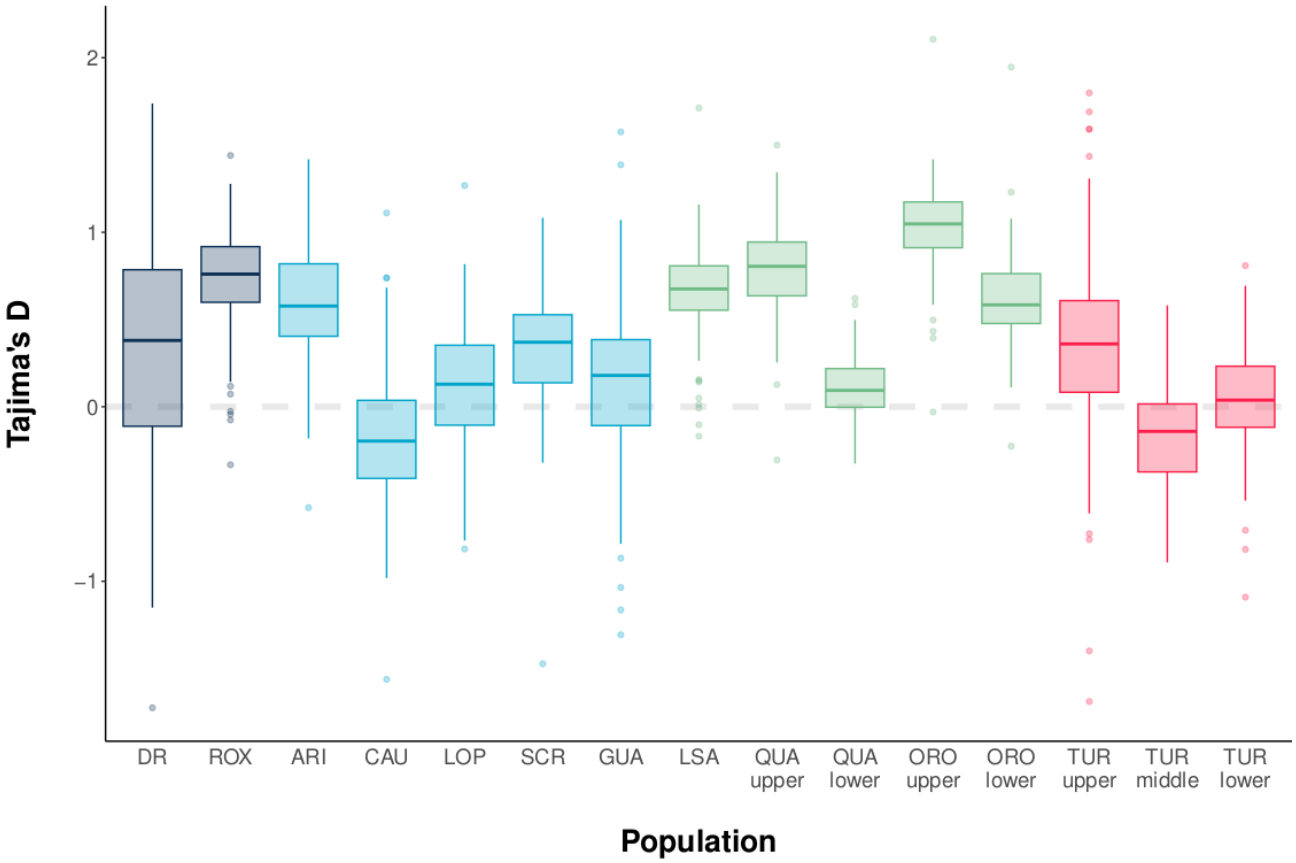

Supplementary Figure 1. Tajima's D in studied populations. The regions are color-coded as follows: Tobago (dark blue), Caroni drainage (light blue), Oropouche drainage (green), Turure river (red).

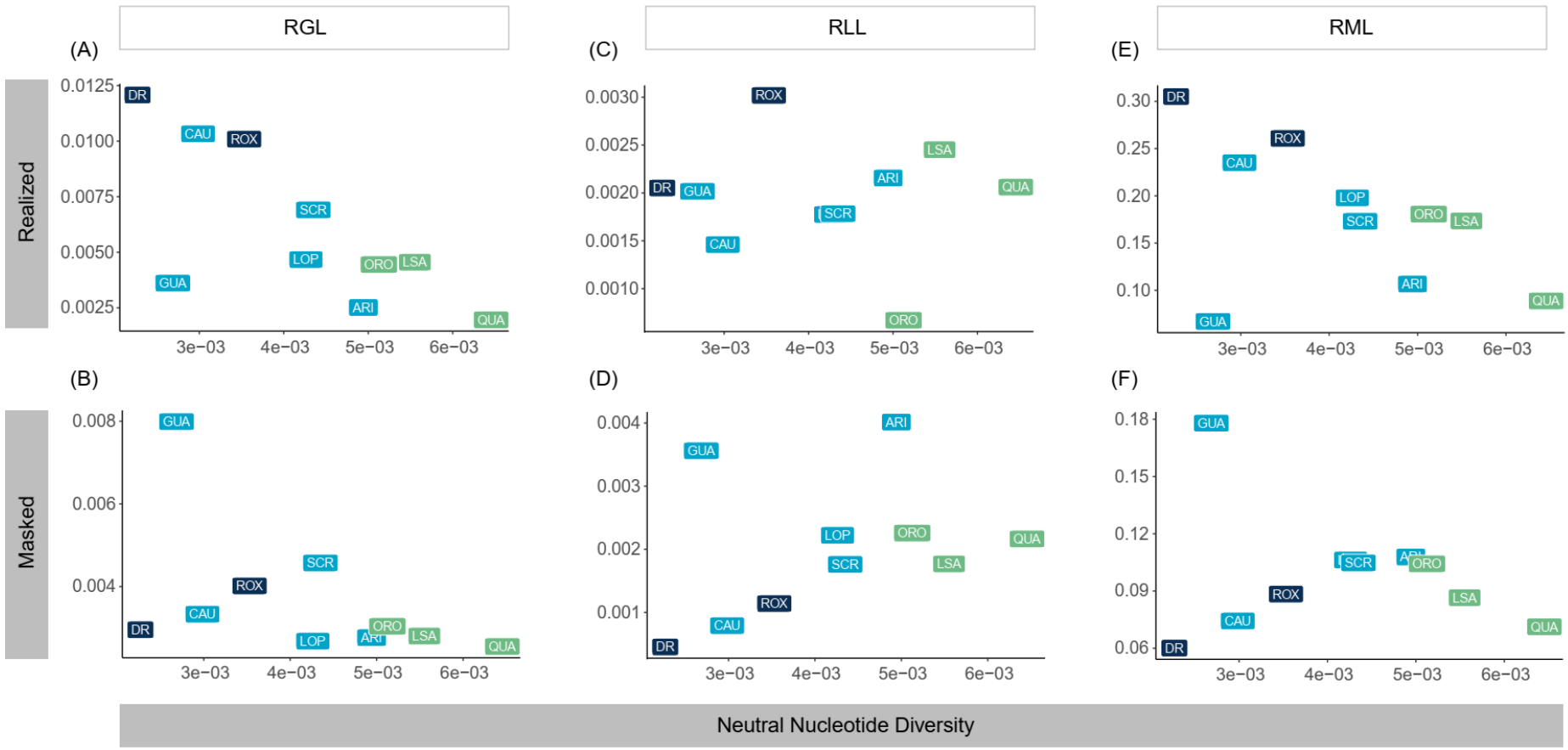

Supplementary Figure 2. Relation between neutral nucleotide diversity and three measures of genetic load in homozygote (Realized) and heterozygote (Masked) genotypes. Left panel represents relative genetic load (RGL), middle panel relative loss-of-function load (RLL) and right panel relative missense load (RML). The regions are colour-coded as follows: Tobago (dark blue), Caroni (light blue) and Oropuche (green).

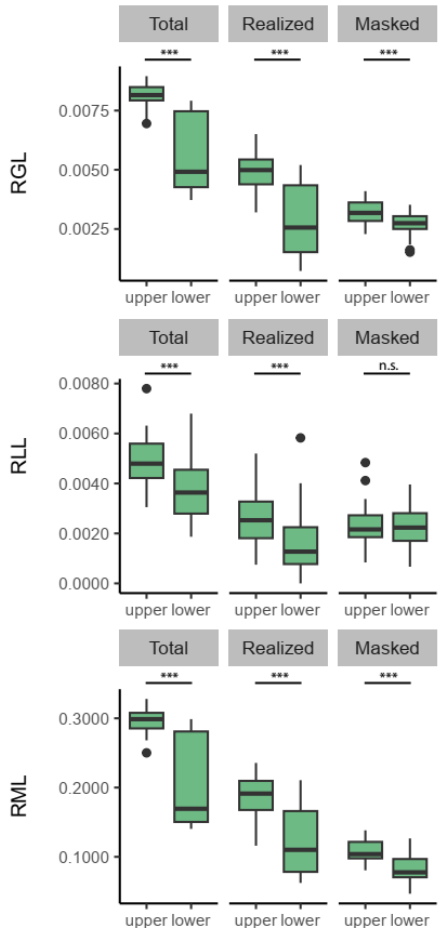

Supplementary Figure 3. Comparisons of load estimates between upper and lower sites of Oropouche and Quare rivers. Top panel represents relative genetic load (RGL), middle panel relative loss-of-function load (RLL) and bottom panel relative missense load (RML). Boxplots drawn from individual-based estimates and horizontal lines with asterixis indicate statistically significant differences.

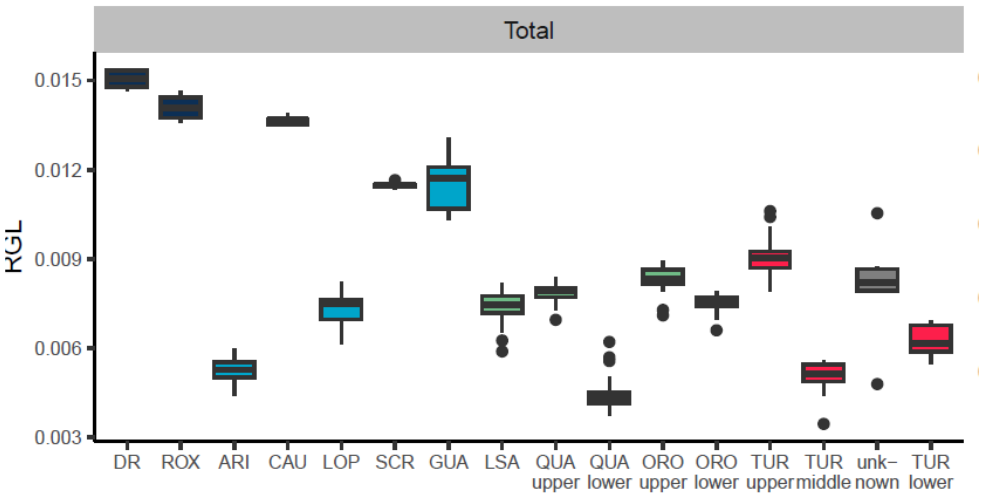

Supplementary Figure 4. Total relative genetic load in all populations. The regions are color-coded as follows: Tobago (dark blue), Caroni (light blue), Oropouche (green), and Turure (red). Gray color shows RGL in individuals of unknown ancestry sampled in Turure middle site.

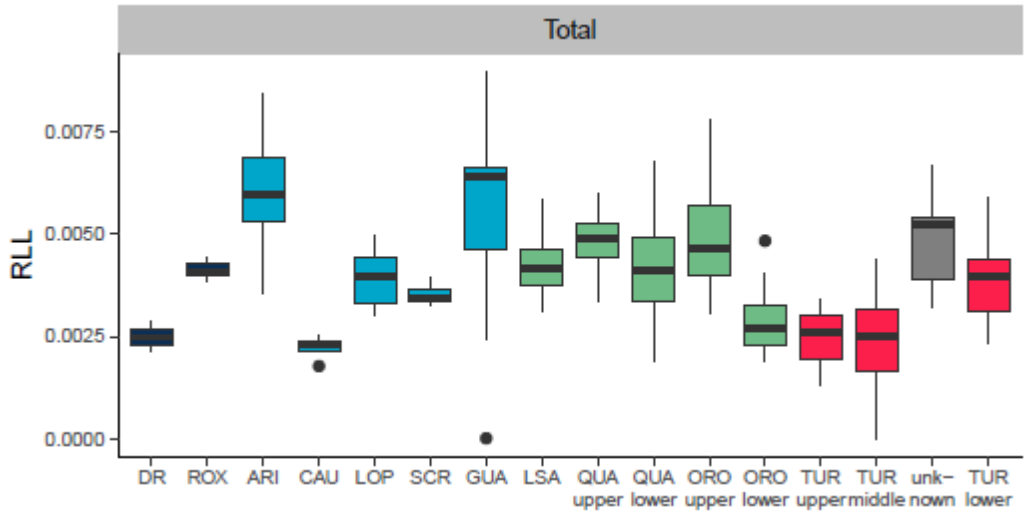

Supplementary Figure 5. Total loss-of-function genetic load in all populations. The regions are color-coded as follows: Tobago (dark blue), Caroni (light blue), Oropouche (green), and Turure (red). Gray color shows RGL in individuals of unknown ancestry sampled in Turure middle site.

Supplementary Tables

Supplementary Table 1. Comparison of genetic load (RGL: relative genetic load; RML: relative missense load; RLL: relative loss of function load) between regions, with estimate of Oropouche in the intercept. Reported statics are t for lms on RGL, z for glms for missense and loss of function. Significant P-values for the region effects are in bold.

Dependent	Predictor	Estimate	SE	statistics	P
Total RGL	intercept	0.0064	0.0016	4.003	<0.001
	Caroni	0.0041	0.0020	2.025	**0.043**
	Tobago	0.0063	0.0025	2.487	**0.013**
log(Masked RGL)	intercept	-5.892	0.1675	-35.18	<0.001
	Caroni	0.2490	0.2126	1.17	0.242
	Tobago	0.4386	0.2680	1.64	0.102
Realized RGL	intercept	-5.721	0.2939	-19.464	<0.001
	Caroni	0.4781	0.3734	1.281	0.2004
	Tobago	0.4715	0.9346	1.982	**0.0475**
Total RML	intercept	-1.4815	0.1004	-14.759	<0.001
	Caroni	0.1621	0.1271	1.276	0.202
	Tobago	0.4523	0.1586	2.852	**0.004**
Masked RML	intercept	-2.4546	0.1300	-18.887	<0.001
	Caroni	0.2334	0.1645	1.419	0.156
	Tobago	-0.1677	0.2055	-0.816	0.414
Realized RML	intercept	-1.9651	0.2128	-9.237	<0.001
	Caroni	0.0241	0.2692	0.089	0.9287
	Tobago	0.7010	0.3363	2.085	**0.0371**
Total RLL	intercept	-5.6073	0.1634	-34.31	<0.001
	Caroni	0.0852	0.2086	0.41	0.683
	Tobago	-0.1305	0.2577	-0.51	0.613
Masked RLL	intercept	-6.1976	0.1039	-59.64	<0.001
	Caroni	0.0369	0.1163	0.32	0.751
	Tobago	-1.0736	0.3488	-3.08	**0.002**
Realized RLL	intercept	-6.4584	0.1805	-35.78	<0.001
	Caroni	0.1322	0.2300	0.57	0.565
	Tobago	0.4673	0.2745	1.70	0.088

Supplementary Table 2. Results of linear models testing the effect of population size, approximated with nucleotide diversity, on three measures of genetic load (RGL: relative genetic load; RML: relative missense load; RLL: relative loss of function load). Significant P-values for the effect of diversity are in bold.

Dependent	Predictor	Estimate	SE	t	P
Total RGL	intercept	0.020	0.002	9.778	<0.001
	diversity	-2.519	0.473	-5.317	**<0.001**
Masked RGL	intercept	0062	0.002	3.75	0.006
	diversity	0.605	0.376	--1.609	0.146
Realized RGL	intercept	0.014	0.003	5.009	0.001
	diversity	1.913671	0.642	2.977	**0.018**
Total RML	intercept	0.415	0.049	8.442	<0.001
	diversity	32.753	11.163	-2.934	**0.019**
Masked RML	intercept	0.117	0.037	3.161	0.013
	diversity	4.532	8.423	0.538	0.605
Realized RML	intercept	0.297	0.076	3.90	0.004
	diversity	28.220	17.314	--1.63	0.142
Total RLL	intercept	0.002	0.001	2.099	0.069
	diversity	0.238	0.316	0.753	0.473
Masked RLL	intercept	0.001	0.001	0.690	0.510
	diversity	0.272	0.279	0.976	0.357
Realized RLL	intercept	0.002	0.001	2.927	0.019
	diversity	0.034	0.161	-0.212	0.837

Supplementary Table 3. Comparison of genetic load (RGL: relative genetic load; RML: relative missense load; RLL: relative loss of function load) of lower (in the intercept) and upper population in Oropouche (in the intercept), and Qare. Reported statistics are t for lms on RGL, z for glms for missense and loss of function. Significant P-values for the effects of the site are in bold. When error distribution was over/under dispersed, quasibinomial distribution was fitted and dispersion parameter (d.p.) is reported in the first column.

Dependent	Predictor	Estimate	SE	statistics	P
Total RGL	intercept	0.0068	0.0002	36.923	<0.001
	site	0.0020	0.0002	10.0	**<0.001**
	population	-0.0018	0.0002	-9.127	<0.001
Masked RGL	intercept	0.0027	0.0001	24.94	<0.001
	site	0.0005	0.0001	3.690	**0.0001**
	population	-0.0001	0.0001	0.672	0.504
Realized RGL	intercept	0.0040	0.0002	19.98	<0.001
	site	0.0016	0.0002	7.13	**<0.001**
	population	-0.0018	0.0002	-8.01	<0.001
Total RML (d.p.=8.92)	intercept	-1.3774	0.0312	-44.03	<0.001
	site	0.2669	0.0353	7.546	**<0.001**
	population	-0.2978	0.0359	-8.294	<0.001
Masked RML (d.p.=6.30)	intercept	-2.4250	0.0407	-59.497	<0.001
	site	0.2104	0.0451	4.670	**<0.001**
	population	-0.0371	0.0450	-0.826	0.412
Realized RML (d.p.= 9.31)	intercept	-1.8120	0.0389	-46.542	<0.001
	site	0.2973	0.0443	6.713	**<0.001**
	population	-0.4601	0.0458	-10.057	<0.001
Total RLL	intercept	-5.73332	0.07904	-72.537	<0.001
	site	0.3307	0.0838	3.945	**<0.001**
	population	0.1568	0.0822	1.907	0.056
Masked RLL	intercept	-6.2279	0.1034	-60.21	<0.001
	site	0.0726	0.1125	0.645	0.5187
	population	0.1860	0.1123	1.657	0.0975
Realized RLL	intercept	-6.6819	0.1236	-54.076	<0.001
	site	0.6452	0.1281	5.036	**<0.001**
	population	0.1232	0.1205	1.022	0.307

Supplementary Table 4. Comparison of genetic load (RGL: relative genetic load; RML: relative missense load; RLL: relative loss of function load) between Guanapo (source population, in the intercept) and upper Turure (translocated population). Reported statistics are t for lms on RGL, z for glms for missense and loss of function. Significant P-values for the population effects are in bold.

Dependent	Predictor	Estimate	SE	t	P
Total RGL	intercept	0.0116	0.0003	44.18	<0.001
	popula-tion	-0.0025	0.0003	-7.76	**<0.0001**
Ln(Masked RGL)	intercept	-2.1061	0.0215	-97.98	<0.001
	popula-tion	-0.2950	0.0265	-11.11	**<0.001**
Realized RGL	intercept	0.0036	0.0004	8.615	<0.001
	popula-tion	0.0014	0.0005	2.857	**0.008**
Total RML	intercept	-1.4209	0.0254	55.895	<0.001
	popula-tion	-0.0766	0.0279	-2.741	**0.006**
Masked RML	intercept	-1.7582	0.0292	-60.13	<0.001
	popula-tion	-0.5723	0.0336	-17.00	**<0.001**
Realized RML (d.p.=3,22)	intercept	-2.6716	0.0792	-33.746	<0.001
	popula-tion	0.6036	0.0835	7.227	**<0.001**
Total RLL	intercept	-5.1974	0.1512	-34.381	<0.001
	popula-tion	-0.8068	0.1813	-4.449	**<0.001**
Masked RLL (d. p. = 0.42)	intercept	-5.6494	0.1228	-46.014	<0.001
	popula-tion	-0.7404	0.1458	-5.077	**<0.001**
Realized RLL	intercept	-6.2090	0.2503	24.81	<0.001
	popula-tion	-0.9346	0.3064	-3.05	**0.0023**

Supplementary Table 5. Comparison of genetic load (RGL: relative genetic load; RML: relative missense load; RLL: relative loss of function load) between Turure upper (in the intercept) and two downstream sites, reported statistics are t for lms on RGL, z for glms for missense and loss of function. Significant P-values for the population effects are in bold.

Dependent	Predictor	Estimate	SE	statistics	P
Total RGL	intercept	0.0091	0.0001	62.28	<0.001
	middle	-0.0041	0.0002	-17.86	**<0.001**
	lower	-0.0028	0.0002	-12.68	**<0.001**
Masked RGL	intercept	0.0039	0.0001	40.917	<0.001
	middle	-0.0011	0.0001	-7.266	**<0.001**
	lower	-0.0003	0.0001	-1.793	0.0799
Realized RGL	intercept	0.0050892	0.0002	31.21	<0.001
	middle	-0.0030	0.0002	-11.63	**<0.001**
	lower	-0.0026	0.0003	-10.27	**<0.001**
Total RML	intercept	-1.4975	0.0116	128.87	<0.001
	middle	-0.4365	0.0254	-17.21	**<0.001**
	lower	-0.1996	0.0191	-10.43	**<0.001**
Masked RML	intercept	-2.3306	0.0167	139.642	<0.001
	middle	-0.2412	0.0344	7.015	**<0.001**
	lower	-0.0019	0.0019	0.071	0.943
Realized RML (d.p.=2.57)	intercept	-2.0680	0.0148	139.45	<0.001
	middle	-0.6177	0.0350	-17.64	**<0.001**
	lower	-0.3836	0.0259	-14.81	**<0.001**
Total RLL	intercept	-6.0041	0.10012	-59.967	<0.001
	middle	-0.0118	0.1908	-0.062	0.950
	lower	0.4379	0.1393	3.144	**0.002**
Masked RLL	intercept	-6.3898	0.1214	-52.647	<0.001
	middle	-0.4912	0.2780	-1.767	0.077
	lower	0.3555	0.1723	2.063	**0.039**
Realized RLL	intercept	-7.1436	0.1768	-40.394	<0.001
	middle	0.5810	0.2771	2.097	**0.0360**
	lower	0.5934	0.2373	2.501	**0.0124**

Supplementary Table 6 Sampling sites on Trinidad and Tobago. The first column is site abbreviation, the 5th, 6th and 7th column is total number of individuals used in this study.

Population	Island	Drainage	Location	N	Males	Females	Juveniles
DR	Tobago	East flowing	N 11.22556 W 060.64500	5	1	4	-
ROX	Tobago	East flowing	N 11.25056 W 060.58250	5	2	3	-
ARI	Trinidad	Caroni	N 10.66969 W 061.22991	14	8	6	-
CAU	Trinidad	Caroni	N 10.70797 W 061.35759	5	2	3	-
LOP	Trinidad	Caroni	N 10.69333 W 061.32195	19	7	12	-
SCR	Trinidad	Caroni	N 10.71565 W 061.46842	5	2	1	2
LSA	Trinidad	Oropouche	N 10.65718 W 061.15276	19	8	11	-
QUA upper	Trinidad	Oropouche	N 10.67610 W 061.19606	11	1	6	4
QUA lower	Trinidad	Oropouche	N 10.65265 W 061.18951	22	7	12	3
ORO upper	Trinidad	Oropouche	N 10.67048 W 061.13784	20	3	3	14
ORO lower	Trinidad	Oropouche	N 10.65963 W 061.13137	13	6	7	-
TUR upper	Trinidad	Oropouche	N 10.67747 W 061.16355	19	8	11	-
TUR middle	Trinidad	Oropouche	N 10.65687 W 061.16776	19	4	15	-
TUR lower	Trinidad	Oropouche	N 10.61899 W 061.15423	14	7	4	3